

# The 2020 United States Decennial Census Is More Private Than You (Might) Think

Buxin Su\*

Weijie J. Su<sup>†</sup>Chendi Wang<sup>‡</sup>

October 10, 2024

## Abstract

The U.S. Decennial Census serves as the foundation for many high-profile policy decision-making processes, including federal funding allocation and redistricting. In 2020, the Census Bureau adopted differential privacy to protect the confidentiality of individual responses through a disclosure avoidance system that injects noise into census data tabulations. The Bureau subsequently posed an open question: Could sharper privacy guarantees be obtained for the 2020 U.S. Census compared to their published guarantees, or equivalently, had the nominal privacy budgets been fully utilized?

In this paper, we affirmatively address this open problem by demonstrating that between 8.50% and 13.76% of the privacy budget for the 2020 U.S. Census remains unused for each of the eight geographical levels, from the national level down to the block level. This finding is made possible through our precise tracking of privacy losses using  $f$ -differential privacy, applied to the composition of private queries across various geographical levels. Our analysis indicates that the Census Bureau introduced unnecessarily high levels of injected noise to achieve the claimed privacy guarantee for the 2020 U.S. Census. Consequently, our results enable the Bureau to reduce noise variances by 15.08% to 24.82% while maintaining the same privacy budget for each geographical level, thereby enhancing the accuracy of privatized census statistics. We empirically demonstrate that reducing noise injection into census statistics mitigates distortion caused by privacy constraints in downstream applications of private census data, illustrated through a study examining the relationship between earnings and education.

## 1 Introduction

The U.S. Census Bureau conducts a decennial national census, with the most recent one held in 2020. The census provides critical information about population distribution, economic indicators, and demographic trends, significantly influencing the nation’s political and economic decisions with consequential and lasting effects. Specifically, the census impacts resource allocation, including federal funding distributions ([Hotchkiss and Phelan, 2017](#)), redistricting ([US Census Bureau, 2023b](#); [Kenny et al., 2023](#); [Cohen et al., 2021](#)), labor markets ([Autor and Duggan, 2003](#); [US Census Bureau, 2021b](#)), and the apportionment of congressional representation ([Eckman, 2021](#); [US Census Bureau, 2021a](#)).

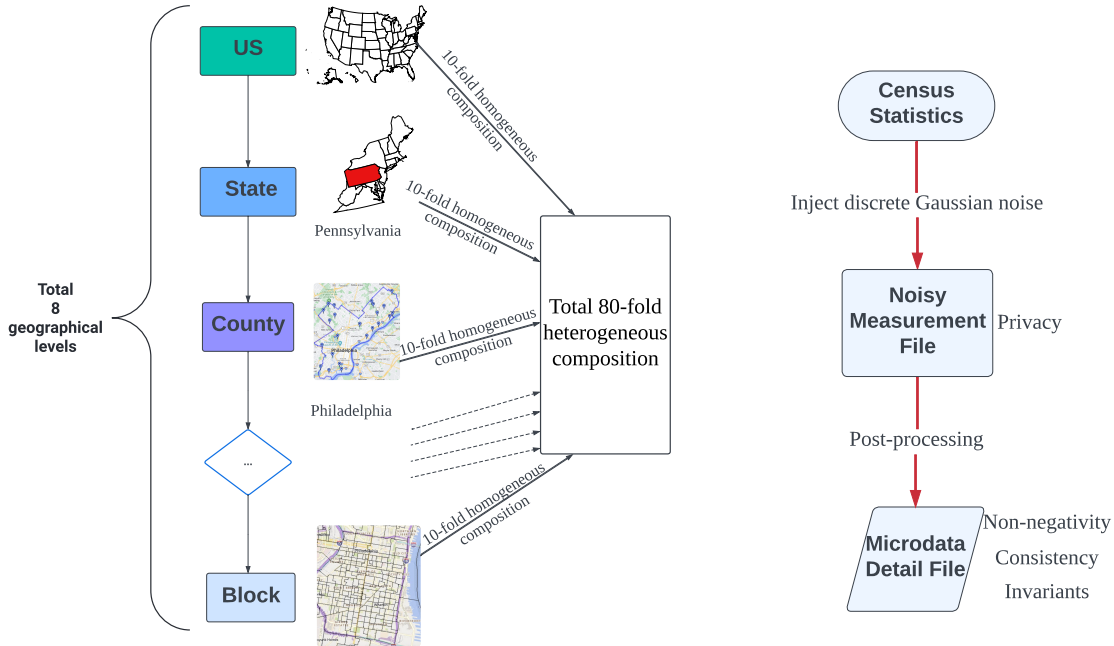
---

\*University of Pennsylvania; Email: [subuxin@sas.upenn.edu](mailto:subuxin@sas.upenn.edu).

<sup>†</sup>University of Pennsylvania; Email: [suw@wharton.upenn.edu](mailto:suw@wharton.upenn.edu).

<sup>‡</sup>Xiamen University; Email: [chendi.wang@xmu.edu.cn](mailto:chendi.wang@xmu.edu.cn).

<sup>§</sup>Authors are listed in alphabetical order.



(a) Composition of the 2020 U.S. Decennial Census.

(b) Privatization and post-processing.

Figure 1: Overview of the disclosure avoidance system (DAS) for the 2020 U.S. Census (Abowd et al., 2022a,b). The omitted geographical levels are tract subset group, tract subset, optimized block group, and population estimates primitive geography (PEPG).

Census data inherently contains sensitive information such as income, race, and age. The direct release of census data, even at the aggregate or summary statistics level, is vulnerable to re-identification and reconstruction attacks, potentially leading to privacy breaches (Duncan and Lambert, 1989; Dick et al., 2023; Hawes, 2022). A notable example is the reconstruction of 46.5% of the population from the 2010 U.S. Census data (Abowd, 2019, 2021). To address the need for privacy and confidentiality in census responses, the U.S. Census Bureau adopted differential privacy (DP)—a privacy-preserving technique with a rigorous mathematical foundation (Dwork et al., 2006b,a)—for the 2020 Census. The implementation was carried out through a disclosure avoidance system (DAS) in the form of a TopDown algorithm (Abowd et al., 2022a,b). This algorithm processes raw census data and injects noise into key tabulations of confidential information. It generates noisy measurement files (NMFs) as intermediate outputs before post-processing, which ensures non-negativity as well as internal and hierarchical consistency. An illustration of the DAS process is provided in Figure 1b.

The injection of noise, whether before or after post-processing, inevitably reduces the accuracy of census data and can lead to undesirable biases against certain subpopulations (Phillips v. US Census Bureau, 2023; Kenny et al., 2021, 2024). Generally, privacy protection affects the reliability of policy-making processes based on census data, such as redistricting, and reduces the accuracy of downstream research on census data (Anderson, 2015; Boyd and Sarathy, 2022; Kenny et al., 2023). Consequently, it is crucial to determine the precise privacy guarantees offered by the DAS for the 2020 Census. If a tighter privacy guarantee than that provided by the Census Bureau can

be established, it would allow less noise to be injected while maintaining the same level of privacy, thereby enhancing census accuracy by fully utilizing the nominal privacy budget. This challenge has been posed as an open problem by the Census Bureau (Kifer et al., 2022) (see its Section 5.2.1).

In this paper, we address the open problem by demonstrating that the 2020 Census offers stronger privacy guarantees than those established by the Census Bureau. Specifically, we prove that, in terms of the privacy parameter  $\epsilon$  in DP—the smaller the  $\epsilon$ , the stronger the privacy guarantee—the 2020 Census has utilized between 86.24% and 91.50% of the privacy budget for each of the eight geographical levels. Put differently, our analysis reveals that the privacy guarantees of the 2020 Census can be improved by 8.50% to 13.76% compared to the nominal privacy guarantees. For instance, at the state level, the Census Bureau’s published value of  $\epsilon$  is 11.07, while our analysis shows that this value can be reduced to 10.13. Importantly, this privacy enhancement comes at no additional cost for any published census data using the Census Bureau’s DAS, as it requires no modification to the current privatization process.

Recognizing these unused privacy guarantees, one could inject less noise into census tabulations, thereby obtaining more accurate NMFs. Indeed, our analysis demonstrates that, under the same privacy budget, the level of noise used by the Census Bureau is unnecessarily high. We have developed a hybrid method combining analytic and computational approaches to efficiently determine the optimal level of injected noise that fully utilizes the privacy budget.<sup>1</sup> For example, our method results in a 20.88% reduction in the variance of injected noise for the national level of the 2020 Census.

The benefit of injecting less noise extends to improved estimation properties after post-processing is applied. Using data from the 2010 U.S. Census across the geographical levels of state, county, tract, and block in Pennsylvania (US Census Bureau, 2022b), our simulation results show that the noise reduction enabled by our analysis decreases the mean squared error (MSE) by approximately 15% when non-negative post-processing is used. The enhanced accuracy of census would naturally improve the reliability of census-based applications. To illustrate this, we conduct an empirical study using data from the ACS 5-year Census (US Census Bureau, 2020e). Our analysis shows that it can significantly mitigate the distortion in estimates caused by the privacy constraints on the data.

The enhanced privacy analysis of the 2020 U.S. Census is made possible by tackling the complex composition structure of the census using the  $f$ -DP framework (Dong et al., 2022). Specifically, the 2020 Census comprises eight geographical levels, with each level containing ten queries (see an illustration in Figure 1a). For each geographical level, the DAS privatizes these queries by adding independent and identically distributed (i.i.d.) integer-valued noise (Canonne et al., 2020). The  $f$ -DP framework is particularly well-suited for precisely accounting for overall privacy loss when composing many steps, each contributing to the privacy loss.

However, a major challenge in applying  $f$ -DP to the 2020 U.S. Census arises from the discreteness of the integer-valued noise used in the DAS, which underlies the technical difficulty of the open problem posed by the Census Bureau (Kifer et al., 2022). The Census Bureau circumvented this challenge by approximating the discrete distribution with its continuous counterpart and using concentrated DP to account for privacy losses (Dwork and Rothblum, 2016; Bun and Steinke, 2016; Bun et al., 2018). While this approximation is a natural choice for concentrated DP, it introduces looseness in the privacy bounds their method can offer. In contrast, our approach directly addresses the discreteness challenge within the  $f$ -DP framework by analytically evaluating the main

---

<sup>1</sup>The code for implementing our method is publicly available on GitHub.

part of the privacy bound while numerically bounding the remainder. Our method, which handles these components separately, presents several technical innovations that might be valuable in other privacy accounting problems where high accuracy is required.

## 2 Results

### 2.1 Preliminaries

To present our main results, we first introduce basic concepts of DP (Dwork et al., 2006b,a). A randomized mechanism  $M$  satisfies  $(\epsilon, \delta)$ -DP for  $\epsilon \geq 0$  and  $0 \leq \delta \leq 1$  if, for any pair of neighboring datasets  $D$  and  $D'$ —where one can be obtained from the other by adding or removing a single individual record—and any event  $S$ , we have

$$\mathbb{P}(M(D) \in S) \leq e^\epsilon \cdot \mathbb{P}(M(D') \in S) + \delta. \tag{2.1}$$

A smaller value of  $\epsilon$  indicates a stronger privacy guarantee. The value of  $\delta$  is typically chosen to be much smaller than the reciprocal of the dataset size (Dwork and Roth, 2014). We refer readers to Kifer et al. (2022) for a semantic interpretation of the parameters  $\epsilon$  and  $\delta$  in the context of census data.

The Census Bureau injected integer-valued noise following the discrete Gaussian distribution into the tabulations of confidential census data. The discrete Gaussian distribution, denoted by  $\mathcal{N}_{\mathbb{Z}}(0, \sigma^2)$ , has a probability mass function given by (Micciancio and Regev, 2007; Canonne et al., 2020)

$$p_\sigma(x) = \frac{e^{-x^2/2\sigma^2}}{\sum_{i \in \mathbb{Z}} e^{-i^2/2\sigma^2}}$$

for any  $x$  in the set of integers  $\mathbb{Z}$ , where  $\sigma > 0$  is the standard deviation.<sup>2</sup>

An important feature of the DAS used in the 2020 Census lies in its composition structure. As illustrated in Figure 1a, the DAS involves eight geographical levels (US Census Bureau, 2022a), with each level releasing ten private queries injected with i.i.d. discrete Gaussian noise. The challenge lies in quantifying the overall privacy loss—in particular, determining the value of  $\epsilon$  in (2.1) for a given  $\delta$ —accumulated across these ten queries.<sup>3</sup> From a technical standpoint, accurately accounting for privacy loss under composition using  $(\epsilon, \delta)$ -DP alone is difficult (Kairouz et al., 2017). The Census Bureau addressed this challenge by using divergence-based relaxations of DP (Dwork and Rothblum, 2016; Bun and Steinke, 2016; Bun et al., 2018; Mironov, 2017) in their privacy accounting method. In contrast, our method employs the more recent  $f$ -DP framework (Dong et al., 2022), developing several novel techniques to handle distributions supported on lattices. The technical details underlying our results are presented in Appendix A.

### 2.2 Improved privacy guarantees at geographical levels

We present our findings in Figure 2, illustrating that the actual privacy guarantee for each geographical level is stronger than those derived using the Census Bureau’s approach. In this analysis,

<sup>2</sup>The variance of  $\mathcal{N}_{\mathbb{Z}}(0, \sigma^2)$  is very close to  $\sigma^2$ . See Appendix A.2.

<sup>3</sup>While there are 50 states, this compositional structure allows us to consider only one state at a time. This is because an individual record would impact at most one state, as different states represent disjoint subsets of the total U.S. population (see more elaboration in McSherry (2010); Smith et al. (2022)).

we adhere to the same configuration of the variances of discrete Gaussian noise added to each level in the DAS (as shown in Table 1). We set  $\delta = 10^{-11}$  for each level, ensuring that the cumulative  $\delta$  across the eight levels does not exceed  $8 \times 10^{-11} < 10^{-10}$ .

The results in Figure 2 show a significant improvement in privacy analysis using our method. The  $\epsilon$  parameter is reduced by a range of 8.50% (at the state level) to 13.76% (at the block level). This finding indicates that the DAS, when applied to the 2020 U.S. Census, has utilized only between 86.24% and 91.50% of the allocated privacy budget for each geographical level.

By varying the value of  $\delta$ , we compare the  $(\epsilon, \delta)$ -curve—also known as the privacy profile (Balle et al., 2020a)—derived from our method with that of the Bureau’s approach at each geographical level. As shown in Figure 3, our method consistently provides a tighter privacy analysis. Furthermore, Figure 7 in Appendix A.5 compares our method using the ACS 5-year estimates (US Census Bureau, 2020a,b,c,d). It demonstrates that our method offers even greater advantages compared to the Bureau’s approach as the number of folds under composition increases.

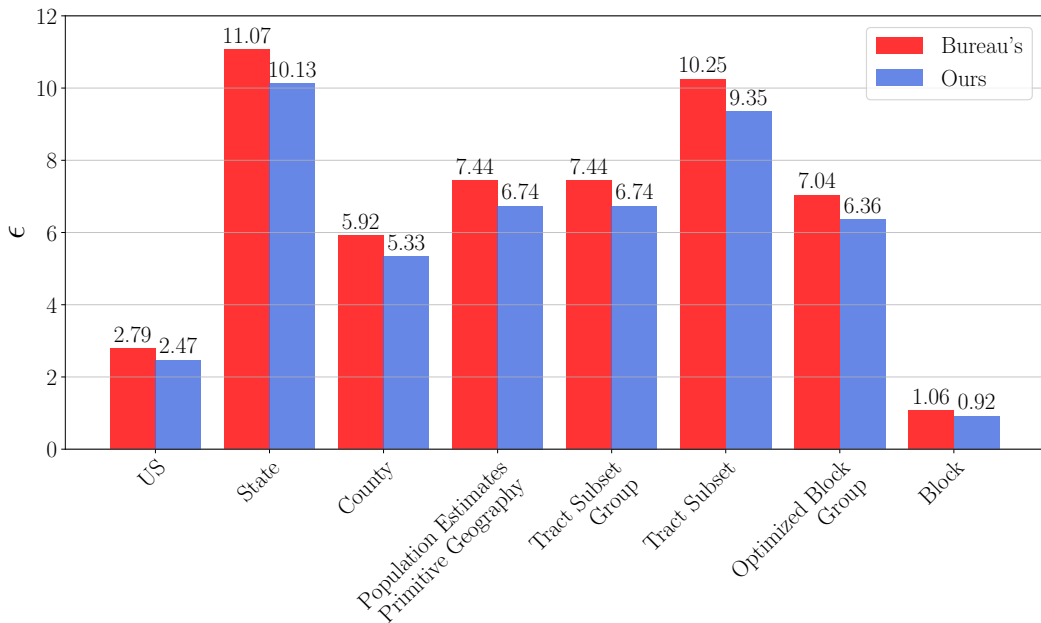


Figure 2: Improved privacy analysis for each geographical level of the 2020 U.S. Census. The red bars represent the Bureau’s original privacy budgets, while the blue bars show the actual privacy parameters ( $\epsilon$ ) calculated using our  $f$ -DP based method, with  $\delta = 10^{-11}$ . The noise configuration follows the privacy-loss budget allocation released on August 25, 2022 by the Bureau (US Census Bureau, 2022a), as detailed in Table 1.

### 2.3 Enhanced accuracy while maintaining the same privacy budget

Using our new method of privacy accounting, the analysis in Section 2.2 implies that noise levels can be reduced while still maintaining the original privacy budget for each geographical level. To achieve the same privacy budget as shown by the red bar in Figure 2 (for example,  $\epsilon = 2.79$  at the national level), we compare the noise levels calculated by our method and the Bureau’s, which are

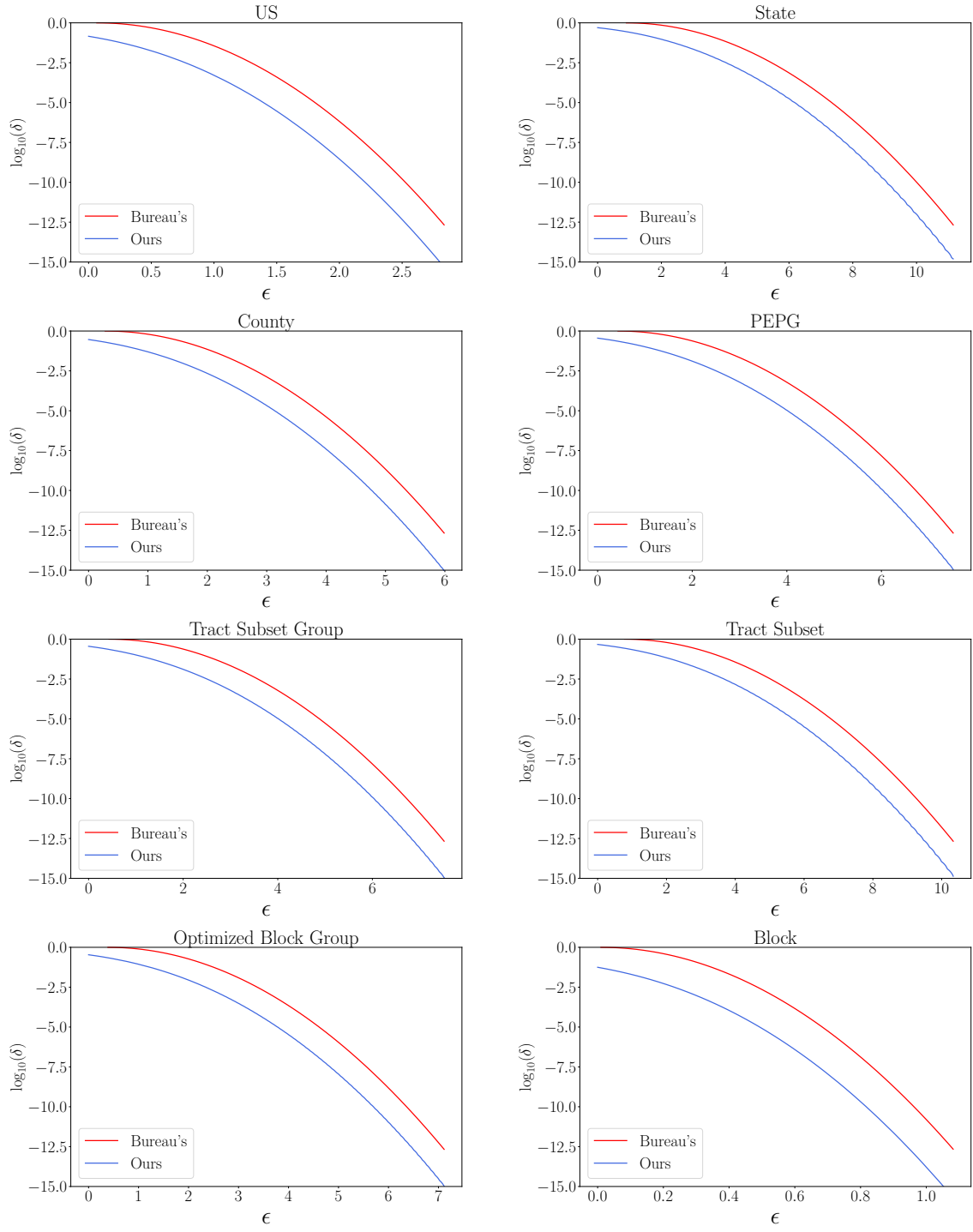


Figure 3: Trade-off between  $\epsilon$  (x-axis) and  $\delta$  (y-axis, logarithmic scale) for each geographical level of the 2020 U.S. Census, using the same setting as Figure 2. Our  $(\epsilon, \delta)$ -curves (blue) consistently lie below those of the Bureau (red), demonstrating that our  $f$ -DP based accounting method achieves improved privacy analysis for any value of  $\delta$ .

displayed in Table 1. The reduction in noise variances is substantial, ranging from 15.08% (national level) to 24.82% (block level).

Formally, the Bureau releases census data by post-processing the NMF through the DAS. To examine how these reduced noise levels translate into improved estimation performance through post-processing, we conduct an analysis using the demographic and housing characteristics file from the 2010 Decennial Census (US Census Bureau, 2022b). Figure 4 shows our results for the geographical levels of state, county, tract, and block in Pennsylvania, comparing the MSE and the mean absolute error (MAE) with the simplest possible post-processing of preserving non-negativity. Without post-processing, our method reduces the MSE by 14.14%, 17.44%, 15.45%, and 24.78%, and the MAE by 7.39%, 9.40%, 8.47%, and 13.26% for the state, county, tract, and block levels, respectively. With non-negative post-processing, the MSE is reduced by 14.01%, 17.31%, 15.21%, and 24.65%, and the MAE by 7.83%, 8.80%, 8.40%, and 13.14%, correspondingly. These results consistently demonstrate that our method can reduce the error introduced by DP constraints, thereby enhancing utility across all geographical levels. Notably, the most significant improvement occurs at the block level, where the noise—and thus the privacy protection—is the greatest.

Geographical levels	US	State	County	PEPG
Bureau’s	68.49	5.00	16.12	10.46
Ours	54.19	4.25	13.28	8.72
Reduction	20.88%	15.08%	17.58%	16.62%
Geographical levels	Tract Subset Group	Tract Subset	Optimized Block Group	Block
Bureau’s	10.46	5.76	11.61	456.62
Ours	8.72	4.87	9.65	343.27
Reduction	16.62%	15.33%	16.89%	24.82%

Table 1: Reduced injected noise for census tabulations while maintaining the same privacy guarantee using our method. The comparison is based on the proxy variance ( $\sigma^2$ ) of the discrete Gaussian noise. The rows corresponding to Bureau’s represent the version of the privacy-loss budget allocation released by the Bureau on August 25, 2022.

## 2.4 Improved overall privacy guarantee

We now consider the overall privacy guarantee across all eight geographical levels. Using the noise levels in Table 1 (the row corresponding to the Bureau’s approach), the Bureau’s calculation of the overall privacy bound using their approach is  $(21.97, 10^{-10})$ -DP. By applying our  $f$ -DP based accounting method, we show that the privacy bound can be improved to  $(20.68, 9.99 \times 10^{-11})$ -DP. In other words, with the same value of  $\delta$  (in fact, slightly smaller), we demonstrate that the total privacy budget  $\epsilon$  can be reduced by 5.15%.

Alternatively, while maintaining the same level of total privacy  $(21.97, 10^{-10})$ -DP across all eight levels, our privacy accounting method allows for the injection of lower levels of noise into each geographical level. Our analysis shows that we can simultaneously reduce the proxy variance parameter  $\sigma^2$  across all geographical levels by 8.59% while maintaining the  $(21.97, 9.99 \times 10^{-11})$ -DP guarantee.



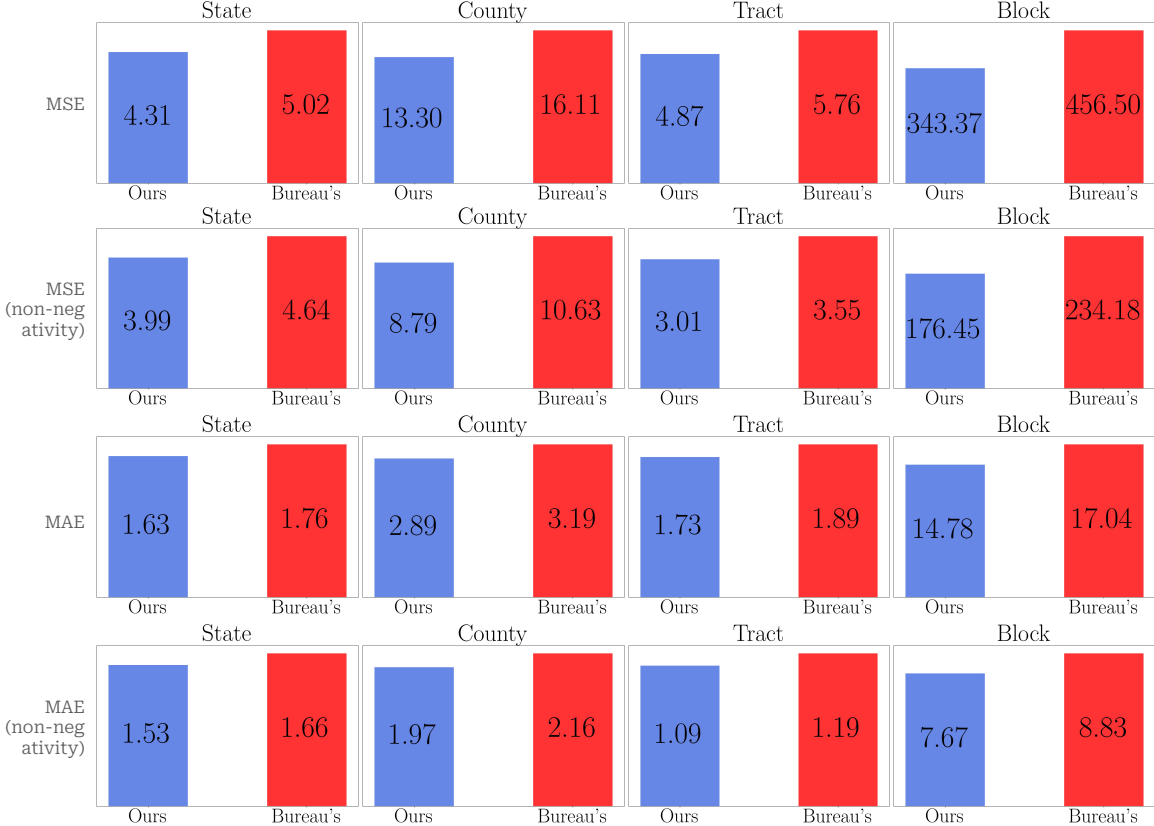


Figure 4: Enhanced accuracy of the 2010 U.S. Census in Pennsylvania, measured by MSE and MAE, with and without non-negativity post-processing. Results are grouped by geographical level. For illustration, only the simplest non-negative post-processing is applied. Noise variances for the discrete Gaussian distribution are as specified in Table 1. Our method (blue) consistently shows lower errors compared to the Bureau’s approach (red) for all geographical levels.

We employ a two-step process to compose the total privacy cost over  $8 \times 10$  folds under composition. The first step, as outlined in Sections 2.2 and 2.3, accounts for the privacy guarantee at each geographical level. For the second step, which aggregates across different levels, a technical challenge arises due to the heterogeneity of injected noise across these levels. We overcome this challenge by leveraging a probabilistic characterization of discrete Gaussian distributions, enabling us to maintain high precision when aggregating across geographical levels. Full technical details are provided in Appendix A.6.

## 2.5 Mitigating distortion in downstream analyses

We examine how our  $f$ -DP based accounting method improves the accuracy and reliability of downstream analyses using census data. The underlying intuition is that, while maintaining the same privacy budget, the use of  $f$ -DP accounting allows for reduced noise added to census counts. To illustrate this, we analyze the relationship between earnings and education level using the 2020 ACS 5-year estimates (US Census Bureau, 2020; Muller, 2002).



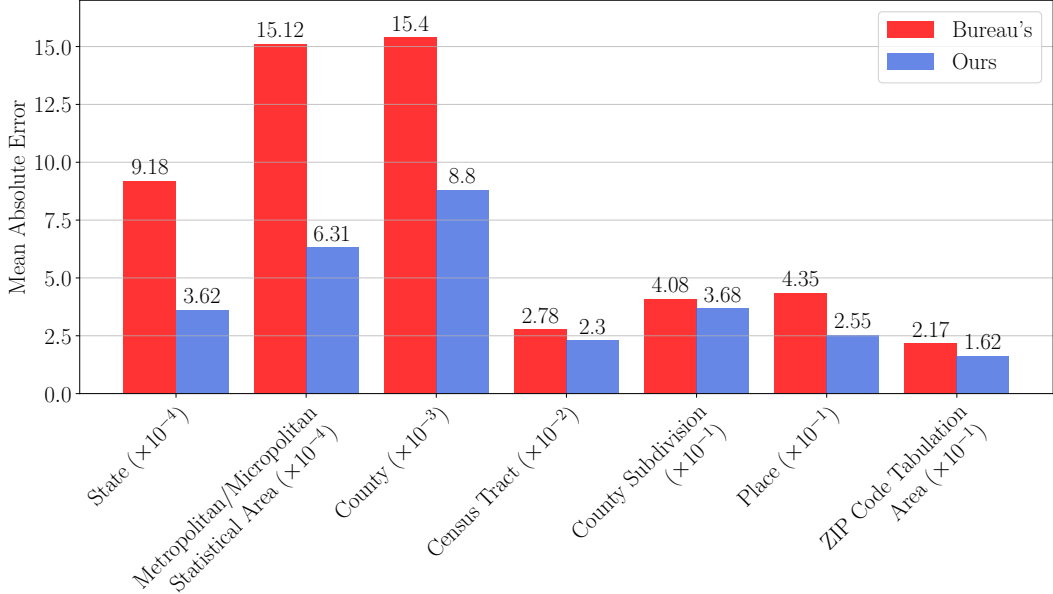


Figure 5: Reduced distortion in estimating the slope coefficient due to privacy constraints for downstream analysis of private census data, measured in terms of MAE (2.2). Noise variances follow the configuration specified in Table 1.

We fit a simple linear regression model of the form  $y = \beta x + \alpha$ , where  $y$  represents the median earnings in a geographical area (state, metropolitan/micropolitan statistical area, county, census tract, county subdivision, place, or ZIP code tabulation area), and  $x$  denotes the proportion of individuals with a bachelor’s degree or higher in the same area. Let  $\hat{\beta}$  be the estimate of the slope coefficient. We then add discrete Gaussian noise with proxy variance parameter  $\sigma^2$  to each of the six education-level categories in the ACS 5-year estimates: less than 9th grade, 9th to 12th grade (no diploma), high school graduate (including equivalency), some college (no degree), associate’s degree, and bachelor’s degree or higher, followed by non-negativity post-processing. Let  $\hat{\beta}_\sigma$  be the slope coefficient obtained by regressing the median earnings  $y$  on the proportion  $x$  computed from the noise-added data.

For a given privacy budget, we determine the proxy standard deviation  $\sigma$  using either our  $f$ -DP accounting method or the Census Bureau’s method. Our approach consistently results in a smaller  $\sigma$  across all possible scenarios. To assess the accuracy of the slope coefficient derived from privatized data, we calculate the MAE between the original slope estimate  $\hat{\beta}$  and its privatized counterpart  $\hat{\beta}_\sigma$ .<sup>4</sup>

$$\frac{1}{K} \sum_{i=1}^K \left| \hat{\beta}_\sigma^{(i)} - \hat{\beta} \right|, \quad (2.2)$$

where  $K$  is the number of independent trials, and  $\hat{\beta}_\sigma^{(i)}$  is the estimate from the  $i$ -th run. Setting  $K = 3$ , Figure 5 demonstrates that our method significantly reduces the distortion of the privatized

<sup>4</sup>It is worth noting that the analyst does not account for the noise distribution in the privatization process. However, the effectiveness of analysis can often be enhanced by incorporating the distribution (see examples in Cumings-Menon (2024); Drechsler et al. (2022); Awan et al. (2024)).

estimates relative to the original estimate at every geographical level, from the state level down to the ZIP code tabulation area. At the state level, for instance, our method reduces the MAE by 60.57% compared to the Bureau’s method.

### 3 Discussion

In this paper, we have analyzed the privacy guarantees of the 2020 U.S. Census relative to the privacy levels published by the Census Bureau. Our analysis demonstrates that the actual privacy guarantee is significantly stronger than that provided by the Bureau’s existing approach. For instance, at the block level, the Bureau’s reported privacy guarantee is  $(1.06, 10^{-11})$ -DP, while our method shows it can be improved to  $(0.92, 10^{-11})$ -DP—an enhancement of 13%—without any changes to the privatization process. This enhanced privacy guarantee applies uniformly for each of the eight geographical levels and all levels combined.

The revelation of this underestimated privacy is made possible through a novel application of the  $f$ -DP framework to the compositional structure of the U.S. Census. Notably, our results address an open problem posed by the U.S. Census Bureau (Kifer et al., 2022). Consequently, our analysis suggests that less noise can be injected into the census data while maintaining the same privacy guarantee. We have empirically demonstrated that this approach would improve the accuracy of census data and significantly reduce distortion due to privacy constraints in downstream analyses. Given the widespread use of census data in fields such as social science (Sullivan, 2020), political science (Ansolabehere and Snyder, 2008; Cohen et al., 2021), and economics (Autor and Duggan, 2003; US Census Bureau, 2021b), we anticipate numerous opportunities to showcase the benefits of this improved privacy-utility trade-off established in our work. Our results further contribute to the growing body of work applying  $f$ -DP to achieve tight privacy accounting for a line of machine learning and data science problems (Bu et al., 2020; Bok et al., 2024; Su, 2024).

Our  $f$ -DP based accounting method is both numerically accurate and computationally efficient when the privacy budget is allocated homogeneously, meaning that the injected discrete Gaussian noise across geographical levels has the same variance. However, both accuracy and computational efficiency degrade for heterogeneous allocations, as evident when comparing the results in Sections 2.2 and 2.4. This degradation stems from the need to address precision issues in floating-point arithmetic (see further discussion in Appendix A.6). To put this into perspective, purely numerical accounting methods (Koskela et al., 2020; Gopi et al., 2021) are computationally infeasible to achieve the same level of accuracy as our method for the 2020 U.S. Census, regardless of whether the allocation is homogeneous or heterogeneous (see elaboration in Appendix A.6). In light of this, an important and challenging direction for future research is to develop privacy accounting methods to better handle heterogeneous privacy budget allocations, where the analytical approaches developed in Kairouz et al. (2021) and Zhu et al. (2022) might offer valuable insights. Alternatively, the Bureau could consider implementing a homogeneous allocation of privacy budget for every geographical level from the outset. Empirical evidence suggests that such homogeneous allocation offers high accuracy when census data is used for redistricting (Cohen et al., 2022).

### Acknowledgments

We thank Simson Garfinkel for valuable information on the implementation of the DAS, and Thomas Steinke for helpful comments. This work was supported in part by NSF DMS-2310679, a Meta Faculty Research Award, and Wharton AI for Business.

## References

- J. Abowd. Declaration of John Abowd in case no. 3: 21-cv-00211-rah-ecm-kcn, the state of alabama v. united states department of commerce, 2021. URL <https://www.documentcloud.org/documents/21018464-fair-lines-america-foundation-july-26-2021-declaration-of-john-m-abowd>.
- J. M. Abowd. Staring down the database reconstruction theorem, 2019. URL <https://www2.census.gov/programs-surveys/decennial/2020/resources/presentations-publications/2019-02-16-abowd-db-reconstruction.pdf>.
- J. M. Abowd, R. Ashmead, R. Cumings-Menon, S. Garfinkel, M. Heineck, C. Heiss, R. Johns, D. Kifer, P. Leclerc, A. Machanavajjhala, et al. The 2020 census disclosure avoidance system TopDown algorithm. *Harvard Data Science Review*, (Special Issue 2), 2022a.
- J. M. Abowd, R. Ashmead, R. Cumings-Menon, S. L. Garfinkel, M. Heineck, C. Heiss, R. Johns, D. Kifer, P. Leclerc, A. Machanavajjhala, B. Moran, W. Sexton, M. Spence, and P. Zhuravlev. Invited lecture: The u.s. census bureau adopts differential privacy. In *KDD '18: Proceedings of the 24th ACM SIGKDD international conference on knowledge discovery & data mining*, 2022b.
- M. J. Anderson. *The American census: A social history*. Yale University Press, 2015.
- S. Ansolabehere and J. Snyder. *The End of Inequality: One Person, One Vote and the Transformation of American Politics*. Issues in American democracy. Norton, 2008. ISBN 9780393931037.
- D. H. Autor and M. G. Duggan. The rise in the disability rolls and the decline in unemployment. *The Quarterly Journal of Economics*, 118(1):157–206, 2003.
- J. Awan, A. Edwards, P. Bartholomew, and A. Sillers. Best linear unbiased estimate from privatized histograms. *arXiv preprint arXiv:2409.04387*, 2024.
- B. Balle, G. Barthe, and M. Gaboardi. Privacy profiles and amplification by subsampling. *J. Priv. Confidentiality*, 10(1), 2020a.
- B. Balle, G. Barthe, M. Gaboardi, J. Hsu, and T. Sato. Hypothesis testing interpretations and renyi differential privacy. In S. Chiappa and R. Calandra, editors, *The 23rd International Conference on Artificial Intelligence and Statistics, AISTATS 2020, 26-28 August 2020, Online [Palermo, Sicily, Italy]*, volume 108 of *Proceedings of Machine Learning Research*, pages 2496–2506. PMLR, 2020b.
- J. Bok, W. J. Su, and J. Altschuler. Shifted interpolation for differential privacy. In *Proceedings of the 41st International Conference on Machine Learning*, volume 235 of *Proceedings of Machine Learning Research*, pages 4230–4266. PMLR, 2024.
- D. Boyd and J. Sarathy. Differential Perspectives: Epistemic Disconnects Surrounding the U.S. Census Bureau’s Use of Differential Privacy. *Harvard Data Science Review*, (Special Issue 2), 2022.
- Z. Bu, J. Dong, Q. Long, and W. J. Su. Deep learning with Gaussian differential privacy. *Harvard Data Science Review*, 2020(23):10–1162, 2020.
- M. Bun and T. Steinke. Concentrated differential privacy: Simplifications, extensions, and lower bounds. In *Theory of Cryptography Conference*, pages 635–658. Springer, 2016.
- M. Bun, C. Dwork, G. N. Rothblum, and T. Steinke. Composable and versatile privacy via truncated CDP. In *Proceedings of the 50th Annual ACM SIGACT Symposium on Theory of Computing*, pages 74–86, 2018.
- C. L. Canonne, G. Kamath, and T. Steinke. The discrete Gaussian for differential privacy. In *Advances in Neural Information Processing Systems*, volume 33, pages 15676–15688. Curran Associates, Inc., 2020.

- A. Cohen, M. Duchin, J. Matthews, and B. Suwal. Census TopDown: The impacts of differential privacy on redistricting. In *2nd Symposium on Foundations of Responsible Computing, FORC 2021, June 9-11, 2021, Virtual Conference*, volume 192 of *LIPICs*, pages 5:1–5:22. Schloss Dagstuhl - Leibniz-Zentrum für Informatik, 2021.
- A. Cohen, M. Duchin, J. Matthews, and B. Suwal. Private Numbers in Public Policy: Census, Differential Privacy, and Redistricting. *Harvard Data Science Review*, (Special Issue 2), 2022.
- R. Cumings-Menon. Full-information estimation for hierarchical data. *arXiv preprint arXiv:2404.13164*, 2024.
- T. Dick, C. Dwork, M. Kearns, T. Liu, A. Roth, G. Vietri, and Z. S. Wu. Confidence-ranked reconstruction of census microdata from published statistics. *Proceedings of the National Academy of Sciences*, 120(8): e2218605120, 2023.
- J. Dong, A. Roth, and W. J. Su. Gaussian differential privacy. *Journal of the Royal Statistical Society: Series B (Statistical Methodology)*, 84(1):3–37, 2022.
- J. Drechsler, I. Globus-Harris, A. Mcmillan, J. Sarathy, and A. Smith. Nonparametric differentially private confidence intervals for the median. *Journal of Survey Statistics and Methodology*, 10(3):804–829, 2022.
- G. Duncan and D. Lambert. The risk of disclosure for microdata. *Journal of Business & Economic Statistics*, 7(2):207–217, 1989.
- R. Durrett. *Probability: theory and examples*, volume 49. Cambridge university press, 2019.
- C. Dwork and A. Roth. The algorithmic foundations of differential privacy. *Foundations and Trends® in Theoretical Computer Science*, 9(3–4):211–407, 2014.
- C. Dwork and G. N. Rothblum. Concentrated differential privacy. *arXiv preprint arXiv:1603.01887*, 2016.
- C. Dwork, K. Kenthapadi, F. McSherry, I. Mironov, and M. Naor. Our data, ourselves: Privacy via distributed noise generation. In *Advances in Cryptology-EUROCRYPT 2006: 24th Annual International Conference on the Theory and Applications of Cryptographic Techniques, St. Petersburg, Russia, May 28-June 1, 2006. Proceedings 25*, pages 486–503. Springer, 2006a.
- C. Dwork, F. McSherry, K. Nissim, and A. Smith. Calibrating noise to sensitivity in private data analysis. *Theory Of Cryptography, Proceedings*, 3876:265–284, 2006b.
- S. J. Eckman. Apportionment and redistricting following the 2020 census. <https://sgp.fas.org/crs/misc/IN11360.pdf>, 2021.
- N. Genise, D. Micciancio, C. Peikert, and M. Walter. Improved discrete gaussian and subgaussian analysis for lattice cryptography. In A. Kiayias, M. Kohlweiss, P. Wallden, and V. Zikas, editors, *Public-Key Cryptography - PKC 2020 - 23rd IACR International Conference on Practice and Theory of Public-Key Cryptography, Edinburgh, UK, May 4-7, 2020, Proceedings, Part I*, volume 12110 of *Lecture Notes in Computer Science*, pages 623–651. Springer, 2020.
- S. Gopi, Y. T. Lee, and L. Wutschitz. Numerical composition of differential privacy. In *Advances in Neural Information Processing Systems 34: Annual Conference on Neural Information Processing Systems 2021, NeurIPS 2021, December 6-14, 2021, virtual*, pages 11631–11642, 2021.
- M. Hawes. Reconstruction and re-identification of the demographic and housing characteristics file (dhc), 2022. URL <https://www2.census.gov/about/partners/cac/sac/meetings/2022-03/presentation-reconstruction-and-reidentification-of-the-dhc.pdf>.

- M. Hotchkiss and J. Phelan. *Uses of Census Bureau data in federal funds distribution: A new design for the 21st century*. United States Census Bureau, 2017.
- P. Kairouz, S. Oh, and P. Viswanath. The composition theorem for differential privacy. *IEEE Trans. Inf. Theory*, 63(6):4037–4049, 2017.
- P. Kairouz, Z. Liu, and T. Steinke. The distributed discrete gaussian mechanism for federated learning with secure aggregation. In *Proceedings of the 38th International Conference on Machine Learning, ICML 2021, 18-24 July 2021, Virtual Event*, volume 139 of *Proceedings of Machine Learning Research*, pages 5201–5212. PMLR, 2021.
- C. T. Kenny, S. Kuriwaki, C. McCartan, E. T. R. Rosenman, T. Simko, and K. Imai. The use of differential privacy for census data and its impact on redistricting: The case of the 2020 U.S. census. *Science Advances*, 7(41):eabk3283, 2021.
- C. T. Kenny, S. Kuriwaki, C. McCartan, E. T. R. Rosenman, T. Simko, and K. Imai. Comment: The Essential Role of Policy Evaluation for the 2020 Census Disclosure Avoidance System. *Harvard Data Science Review*, (Special Issue 2), 2023.
- C. T. Kenny, C. McCartan, T. Simko, and K. Imai. Census officials must constructively engage with independent evaluations. *Proceedings of the National Academy of Sciences*, 121(11):e2321196121, 2024.
- D. Kifer, J. M. Abowd, R. Ashmead, R. Cumings-Menon, P. Leclerc, A. Machanavajjhala, W. Sexton, and P. Zhuravlev. Bayesian and frequentist semantics for common variations of differential privacy: Applications to the 2020 census. *arXiv preprint arXiv:2209.03310*, 2022.
- A. Koskela, J. Jälkö, and A. Honkela. Computing tight differential privacy guarantees using FFT. In *The 23rd International Conference on Artificial Intelligence and Statistics, AISTATS 2020, 26-28 August 2020, Online [Palermo, Sicily, Italy]*, volume 108 of *Proceedings of Machine Learning Research*, pages 2560–2569. PMLR, 2020.
- E. L. Lehmann and J. P. Romano. *Testing statistical hypotheses*. Springer Texts in Statistics. Springer, New York, third edition, 2005. ISBN 0-387-98864-5.
- F. McSherry. Privacy integrated queries: an extensible platform for privacy-preserving data analysis. *Commun. ACM*, 53(9):89–97, 2010.
- D. Micciancio and O. Regev. Worst-case to average-case reductions based on Gaussian measures. *SIAM Journal on Computing*, 37(1):267–302, 2007.
- I. Mironov. Rényi differential privacy. In *2017 IEEE 30th computer security foundations symposium (CSF)*, pages 263–275. IEEE, 2017.
- A. Muller. Education, income inequality, and mortality: a multiple regression analysis. *BMJ*, 324(7328):23, 2002.
- Phillips v. US Census Bureau. Phillips v. U.S. Census Bureau. <https://thearp.org/litigation/phillips-v-us-census-bureau/>, 2023.
- P. Sablonnière, D. Sibih, and M. Tahrchi. Error estimate and extrapolation of a quadrature formula derived from a quartic spline quasi-interpolant. *BIT*, 50(4):843–862, 2010. ISSN 0006-3835.
- J. Smith, H. J. Asghar, G. Gioiosa, S. Mrabet, S. Gaspers, and P. Tyler. Making the most of parallel composition in differential privacy. *Proc. Priv. Enhancing Technol.*, 2022(1):253–273, 2022.

- W. J. Su. A statistical viewpoint on differential privacy: Hypothesis testing, representation and Blackwell’s theorem. *arXiv preprint arXiv:2409.09558*, 2024.
- T. A. Sullivan. Coming to Our Census: How Social Statistics Underpin Our Democracy (and Republic). *Harvard Data Science Review*, 2(1), 2020.
- US Census Bureau. Selected social characteristics in the united states. U.S. Census Bureau, 2020a. URL <https://data.census.gov/table/ACSDP5Y2020.DP02?y=2020&d=ACS5-YearEstimatesDataProfiles>. Accessed on 4 October 2024.
- US Census Bureau. Selected economic characteristics. U.S. Census Bureau, 2020b. URL <https://data.census.gov/table/ACSDP5Y2020.DP03?y=2020&d=ACS5-YearEstimatesDataProfiles>. Accessed on 4 October 2024.
- US Census Bureau. Selected housing characteristics. U.S. Census Bureau, 2020c. URL <https://data.census.gov/table/ACSDP5Y2020.DP04?y=2020&d=ACS5-YearEstimatesDataProfiles>. Accessed on 4 October 2024.
- US Census Bureau. Acs demographic and housing estimates. U.S. Census Bureau, 2020d. URL <https://data.census.gov/table/ACSDP5Y2020.DP05?y=2020&d=ACS5-YearEstimatesDataProfiles>. Accessed on 4 October 2024.
- US Census Bureau. Educational attainment. U.S. Census Bureau, 2020e. URL [https://data.census.gov/table/ACSST5Y2020.S1501?q=S1501&g=010XX00US\\$0400000](https://data.census.gov/table/ACSST5Y2020.S1501?q=S1501&g=010XX00US$0400000).
- US Census Bureau. 2020 census apportionment results. <https://www.census.gov/data/tables/2020/dec/2020-apportionment-data.html>, 2021a.
- US Census Bureau. Guidance for labor force statistics data users. <https://www.census.gov/topics/employment/labor-force/guidance.html>, 2021b.
- US Census Bureau. Privacy-loss budget allocation 2022-08-25. [https://www2.census.gov/programs-surveys/decennial/2020/program-management/data-product-planning/2010-demonstration-data-products/02-Demographic\\_and\\_Housing\\_Characteristics/2022-08-25\\_Summary\\_File/2022-08-25\\_Privacy-Loss\\_Budget\\_Allocations.pdf](https://www2.census.gov/programs-surveys/decennial/2020/program-management/data-product-planning/2010-demonstration-data-products/02-Demographic_and_Housing_Characteristics/2022-08-25_Summary_File/2022-08-25_Privacy-Loss_Budget_Allocations.pdf), 2022a.
- US Census Bureau. Privacy-protected 2010 census demonstration data — ipums nhgis. <https://www.nhgis.org/privacy-protected-2010-census-demonstration-data#v20220825-files>, 2022b.
- US Census Bureau. DAS-implementation-details. U.S. Census Bureau, 2023a. URL [https://github.com/uscensusbureau/DAS\\_2020\\_DHC\\_Production\\_Code/blob/main/wiki/DAS-Implementation-Details.md](https://github.com/uscensusbureau/DAS_2020_DHC_Production_Code/blob/main/wiki/DAS-Implementation-Details.md).
- US Census Bureau. Census bureau data guide more than \$2.8 trillion in federal funding in fiscal year 2021, 2023b. URL <https://www.census.gov/newsroom/press-releases/2023/decennial-census-federal-funds-distribution.html>.
- C. Wang, B. Su, J. Ye, R. Shokri, and W. J. Su. Unified enhancement of privacy bounds for mixture mechanisms via  $f$ -differential privacy. *Advances in Neural Information Processing Systems*, 36, 2024.
- H. Wang, S. Gao, H. Zhang, M. Shen, and W. J. Su. Analytical composition of differential privacy via the Edgeworth accountant. *arXiv preprint arXiv:2206.04236*, 2022.
- Y. Zhu, J. Dong, and Y.-X. Wang. Optimal accounting of differential privacy via characteristic function. In *International Conference on Artificial Intelligence and Statistics*, pages 4782–4817. PMLR, 2022.

## A Technical proofs and details

This section presents our main methodology and key tools for deriving the privacy profile of the U.S. Census. Section A.1 provides an overview of differential privacy. Section A.2 summarizes technical facts about discrete Gaussian distributions used to bound approximation errors. In Section A.3, we present  $f$ -DP guarantees for the discrete Gaussian mechanisms and discuss the challenge of deriving the exact privacy profile under composition. Section A.4 describes our approach to approximating the privacy profile for i.i.d. DGMs, with the approximation error analyzed in Section A.5. Section A.6 examines the composition of heterogeneous DGMs used to allocate the privacy budget across eight geographical levels.

### A.1 Preliminaries on differential privacy

In this section, we discuss the basics of differential privacy (Dwork et al., 2006b,a) and its application in protecting the U.S. Census using the discrete Gaussian mechanism (Canonne et al., 2020).

Let  $\mathcal{X}$  represent the sample space, and let  $D \subset \mathcal{X}^m$  be a dataset containing  $m$  data records. Consider a deterministic query  $M : \mathcal{X}^m \rightarrow \mathbb{Z}^d$  that takes only integer values. To ensure privacy, the discrete Gaussian mechanism (DGM), which adds discrete Gaussian noise to  $M$ , is employed within the DAS. Recall the discrete Gaussian distribution given in Section 2. The DGM takes each query  $M(D)$  as an input and outputs the privatized query

$$\widetilde{M}(D) = M(D) + \mathcal{N}_{\mathbb{Z}}(0, \sigma^2). \quad (\text{A.1})$$

The privacy budget for the 2020 U.S. Census is measured using zero-Concentrated Differential Privacy (zCDP) (Bun and Steinke, 2016), which is based on Rényi divergence. For two distributions,  $P$  and  $Q$ , with probability density functions  $p$  and  $q$ , respectively, the Rényi divergence of order  $\alpha > 1$  is defined as  $R_\alpha(P\|Q) = \frac{1}{\alpha-1} \log \int p(x)^\alpha q(x)^{1-\alpha} dx$ .  $R_1(P\|Q)$  or  $R_\infty(P\|Q)$  is the limit of  $R_\alpha(P\|Q)$  as  $\alpha$  tends to 1 or infinity, respectively. Based on the Rényi divergence, one has the following definition of zCDP. Here, the Rényi divergence between two random variables is understood as the divergence between their respective distributions.

**Definition A.1** (zCDP, Bun and Steinke (2016)). A randomized mechanism  $\widetilde{M}$  is said to satisfy  $\rho$ -zCDP if

$$R_\alpha(\widetilde{M}(D)\|\widetilde{M}(D')) \leq \rho\alpha, \quad \text{for all } \alpha > 1,$$

and for any neighboring datasets  $D$  and  $D'$ .

Another key aspect related to the privacy budget is the sensitivity of each query. For a query  $M$  taking values in  $\mathbb{R}^d$ , the  $l_2$ -sensitivity of  $M$  is defined as

$$\Delta_M = \sup_{D, D'} \left\{ \|M(D) - M(D')\|_{\ell_2} \right\},$$

where  $\|\cdot\|_{\ell_2}$  is the  $\ell_2$ -norm of a vector and the supremum is taken over all datasets  $D$  and  $D'$  that differ in at most one data record.

In the implementation of the TopDown algorithm (US Census Bureau, 2023a), an add/delete sensitivity of 1 is used. This reflects the difference between two neighboring datasets when a single



data record is added or removed. The underlying theory of the DAS (Abowd et al., 2022a) considers a broader sensitivity model that also accounts for replacing one record with another, resulting in a sensitivity of up to  $\sqrt{2}$  for coarsened counting queries with binary categories (e.g., “18 and older” vs. “17 and younger”). We adopt the add/delete sensitivity of 1, corresponding to the unbounded case in the actual implementation (US Census Bureau, 2023a). Our method can be naturally extended to the replacement case (yielding a sensitivity of  $\sqrt{2}$ ) by treating the binary categories as the 2-fold composition of two counting queries.

According to Canonne et al. (2020), the discrete Gaussian mechanism is  $\rho$ -zCDP if we take  $\sigma^2 = \Delta_M^2/2\rho$ . zCDP is currently adopted by the Bureau to count the privacy budget of the Census 2020. A better zCDP guarantee for the discrete Gaussian is also investigated by Kairouz et al. (2021). The Bureau obtained the privacy budget  $(\epsilon, \delta)$  for the Census by converting  $\rho$ -zCDP to  $(\epsilon, \delta)$ -DP using the following equation from Bun et al. (2018):

$$\epsilon = \rho + 2\sqrt{-\rho \log \delta}.$$

However, zCDP may provide a loose privacy profile due to the inherent looseness of the Rényi divergence (Balle et al., 2020b). In this paper, we aim to provide an  $f$ -DP guarantee for the DGM, which is known to be tight (Dong et al., 2022; Wang et al., 2024). Under the setting of  $f$ -DP, the distinguishability between  $\widetilde{M}(D)$  and  $\widetilde{M}(D')$  can be quantified using hypothesis testing (Kairouz et al., 2017; Dong et al., 2022). Consider a hypothesis testing problem  $H_0 : P$  v.s.  $H_1 : Q$  and a rejection rule  $\phi \in [0, 1]$ . We define the type I error as  $\alpha_\phi = \mathbb{E}_P[\phi]$ , which is the probability of incorrectly rejecting the null hypothesis  $H_0$ . The type II error  $\beta_\phi = 1 - \mathbb{E}_Q[\phi]$  is the probability that we accept the alternative  $H_1$  wrongly.

The trade-off function  $T(P, Q)$  is the minimal type II error at a given level  $\alpha$  of the type I error, that is,

$$T(P, Q)(\alpha) = \inf_{\phi} \{\beta_\phi : \alpha_\phi \leq \alpha\},$$

where the infimum is taken over all rejection rule  $\phi$ . According to the Neyman–Pearson lemma (cf., Lehmann and Romano, 2005), the infimum is achieved by the likelihood ratio test. For any two random variables  $\xi$  and  $\zeta$ , we define  $T(\xi, \zeta)$  as the trade-off function between the respective distributions.

**Definition A.2** ( $f$ -DP). We say a mechanism  $\widetilde{M}$  satisfies  $f$ -DP if  $T(\widetilde{M}(D), \widetilde{M}(D'))(\alpha) \geq f(\alpha)$  for any  $\alpha \in [0, 1]$  and any neighboring datasets  $D$  and  $D'$ .

$f$ -DP is equivalent to  $(\epsilon, \delta(\epsilon))$ -DP for all  $\epsilon > 0$  according to Proposition 2.12 in Dong et al. (2022).

## A.2 Useful facts for discrete Gaussian distributions

In this section, we introduce several useful facts about discrete Gaussian distributions, including the sub-Gaussian tail bound and properties of the characteristic functions. Proofs for these results are deferred to Section B.

**Sub-Gaussian properties of discrete Gaussian distributions.** Let  $X_i \sim \text{i.i.d. } \mathcal{N}_{\mathbb{Z}}(0, \sigma^2)$  and define  $S_n = \frac{1}{B_n} \sum_{i=1}^n X_i$ , where  $B_n = \sqrt{n}\sigma$ . According to Corollary 17 in [Canonne et al. \(2020\)](#),  $X_i$  is sub-Gaussian with variance proxy  $\sigma^2$ . Therefore,  $S_n$  is the sum of  $n$  i.i.d. sub-Gaussian random variables, each with a variance proxy of  $\sigma^2$ , and is thus sub-Gaussian with variance proxy  $n\sigma^2$ . Specifically, it holds

$$\mathbb{P}(S_n > m_1) = \mathbb{P}\left(\sum_{i=1}^n X_i > m_1 B_n\right) \leq e^{-\frac{(m_1 B_n)^2}{2n\sigma^2}} = e^{-\frac{m_1^2}{2}}, \quad (\text{A.2})$$

for any  $m_1 > 0$ .

**Variance of discrete Gaussian distributions.** For any variance proxy  $\sigma^2$  used by the Bureau (the row corresponding to Bureau's) in Table 1, the variance of  $\mathcal{N}_{\mathbb{Z}}(0, \sigma^2)$  is close to  $\sigma^2$ .

**Fact A.3.** The variance of  $\mathcal{N}_{\mathbb{Z}}(0, \sigma^2)$  is bounded as follows: For any  $4.25 \leq \sigma^2 \leq 5.00$ ,

$$\sigma^2 - 5.8 \times 10^{-34} < \text{Var}(\mathcal{N}_{\mathbb{Z}}(0, \sigma^2)) < \sigma^2.$$

For any  $5.00 < \sigma^2 \leq 10.00$ ,

$$\sigma^2 - 2.8 \times 10^{-40} < \text{Var}(\mathcal{N}_{\mathbb{Z}}(0, \sigma^2)) < \sigma^2.$$

For any  $\sigma^2 > 10.00$ ,

$$\sigma^2 - 1.5 \times 10^{-82} < \text{Var}(\mathcal{N}_{\mathbb{Z}}(0, \sigma^2)) < \sigma^2.$$

The following characteristic function of  $S_n$  will be used to investigate the privacy profile of the DGM.

**Characteristic functions of  $S_n$ .** The characteristic function of  $S_n$  can be represented as follows:

$$\begin{aligned} f_{S_n}(t) &= \mathbb{E}e^{itS_n} = \left( \frac{\sum_{u=-\infty}^{\infty} e^{-u^2/2\sigma^2} e^{i \cdot t/B_n \cdot u}}{\sum_{u=-\infty}^{\infty} e^{-u^2/2\sigma^2}} \right)^n \\ &\stackrel{(a)}{=} \left( \frac{\sum_{u=-\infty}^{\infty} e^{-\sigma^2(t/B_n - 2\pi u)^2/2}}{\sum_{u=-\infty}^{\infty} e^{-2\sigma^2\pi^2 u^2}} \right)^n \\ &= \left( e^{-\frac{t^2}{2n}} \cdot \frac{\theta_3\left(-i\sigma\pi t/\sqrt{n}, e^{-2\sigma^2\pi^2}\right)}{\theta_3\left(0, e^{-2\sigma^2\pi^2}\right)} \right)^n \\ &= e^{-t^2/2} \left( \frac{\theta_3\left(-i\sigma\pi t/\sqrt{n}, e^{-2\sigma^2\pi^2}\right)}{\theta_3\left(0, e^{-2\sigma^2\pi^2}\right)} \right)^n, \end{aligned} \quad (\text{A.3})$$

where  $\theta_3(u, q) = 1 + 2 \sum_{k=1}^{\infty} q^{k^2} \cos(2ku)$  is a theta function and Equation (a) holds due to Poisson summation formula.

To characterize the maximum value and monotonicity of  $f_{S_n}(t)$ , we use the following lemma.

**Lemma A.4.** For any  $0 \leq \mu < \nu \leq \frac{1}{2}$ , we have  $\sum_{x \in \mathbb{Z}} e^{-\frac{(x-\mu)^2}{2\sigma^2}} > \sum_{x \in \mathbb{Z}} e^{-\frac{(x-\nu)^2}{2\sigma^2}}$ .

As a direct consequence of Lemma A.4, the derivative of  $\sum_{x \in \mathbb{Z}} e^{-\frac{(x-\mu)^2}{2\sigma^2}}$  with respect to  $\mu \in (0, 1/2)$  is negative. That is, it holds

$$\frac{d}{d\mu} \sum_{x \in \mathbb{Z}} e^{-\frac{(x-\mu)^2}{2\sigma^2}} < 0, \quad \text{for } \mu \in (0, 1/2). \quad (\text{A.4})$$

**Proposition A.5** (Correction to Fact 18 in [Canonne et al. \(2020\)](#)). The DGM is unbiased in the sense that  $\mathbb{E} \mathcal{N}_{\mathbb{Z}}(\mu, \sigma^2) = \mu$  if and only if  $\mu \in \frac{1}{2}\mathbb{Z}$ .

*Proof.* By Lemma A.4, we have

$$\mathbb{E} \mathcal{N}_{\mathbb{Z}}(\mu, \sigma^2) - \mu = \sum_{x \in \mathbb{Z}} (x - \mu) e^{-\frac{(x-\mu)^2}{2\sigma^2}} = \sigma^2 \cdot \frac{d}{d\mu} \sum_{x \in \mathbb{Z}} e^{-\frac{(x-\mu)^2}{2\sigma^2}} < 0,$$

for any  $0 < \mu < 1/2$ . This completes the proof.  $\square$

Using Lemma A.4, we derive the following properties of  $f_{S_n}$  which will be essential in proving Fact C.1.

**Proposition A.6.** The characteristic function  $f_{S_n}(t)$  is periodic with period  $2\pi B_n$ . Moreover,  $f_{S_n}(t)$  is strictly increasing on  $(-\pi B_n, 0)$  and is strictly decreasing on  $(0, \pi B_n)$ . Consequently,  $f_{S_n}(t)$  achieves its maximum at  $t = 0$  with a maximum value of  $f_{S_n}(0) = 1$ .

### A.3 $f$ -DP guarantees for discrete Gaussian mechanisms

From an  $f$ -DP perspective, for two neighboring datasets  $D$  and  $D'$ , the privacy of the discrete Gaussian mechanisms is to test

$$H_0 : \widetilde{M}(D) = M(D) + \mathcal{N}_{\mathbb{Z}}(0, \sigma^2) \quad \text{v.s.} \quad H_1 : \widetilde{M}(D') = M(D') + \mathcal{N}_{\mathbb{Z}}(0, \sigma^2).$$

For integer-valued queries  $M(D)$  and  $M(D')$ ,  $f$ -DP provides a tight privacy profile of the DGM (without composition). First, we have

$$\begin{aligned} T(\mathcal{N}_{\mathbb{Z}}(M(D), \sigma^2), \mathcal{N}_{\mathbb{Z}}(M(D'), \sigma^2)) &= T(\mathcal{N}_{\mathbb{Z}}(0, \sigma^2), \mathcal{N}_{\mathbb{Z}}(M(D') - M(D), \sigma^2)) \\ &\geq T(\mathcal{N}_{\mathbb{Z}}(0, \sigma^2), \mathcal{N}_{\mathbb{Z}}(\mu, \sigma^2)), \end{aligned}$$

where  $\mu \in \mathbb{Z}$  is the sensitivity of  $M$ . Therefore, it is sufficient to evaluate  $T(X, X + \mu)$  for  $X \sim \mathcal{N}_{\mathbb{Z}}(0, \sigma^2)$ . Let  $\Phi_{\mathbb{Z}, \sigma}$  and  $\phi_{\mathbb{Z}, \sigma}$  be the cumulative distribution function (cdf) and probability mass function (pmf) of  $\mathcal{N}_{\mathbb{Z}}(0, \sigma^2)$ , respectively. We then have the following  $f$ -DP guarantee for the discrete Gaussian mechanisms.

**Theorem A.7.** For  $\mu \in \mathbb{Z}$  and  $X \sim \mathcal{N}_{\mathbb{Z}}(0, \sigma^2)$ , we have

$$T(X, X + \mu)(\alpha) = \Phi_{\mathbb{Z}, \sigma}(\Phi_{\mathbb{Z}, \sigma}^{-1}(1 - \alpha) - \mu) - \frac{\varphi_{\mathbb{Z}, \sigma}(t_\alpha - \mu)}{\varphi_{\mathbb{Z}, \sigma}(t_\alpha)} (\alpha + \Phi_{\mathbb{Z}, \sigma}(t_\alpha) - 1),$$

where  $t_\alpha = \Phi_{\mathbb{Z}, \sigma}^{-1}(1 - \alpha) \in \mathbb{Z}$ . In particular, for each knot  $\alpha$  such that  $1 - \alpha = \Phi_{\mathbb{Z}, \sigma}(\Phi_{\mathbb{Z}, \sigma}^{-1}(1 - \alpha))$  (i.e.,  $1 - \alpha \in \Phi_{\mathbb{Z}, \sigma}(\mathbb{Z})$ ), it holds

$$T(X, X + \mu)(\alpha) = \Phi_{\mathbb{Z}, \sigma}(\Phi_{\mathbb{Z}, \sigma}^{-1}(1 - \alpha) - \mu).$$

*Proof.* For simplicity, we prove the case  $\sigma = 1$  and the general case can be derived similarly. We have

$$\alpha(t) = \mathbb{P}[X > t] + c\varphi_{\mathbb{Z}}(t) = 1 - \Phi_{\mathbb{Z}}(t_{\alpha}) + c_{\alpha}\varphi_{\mathbb{Z}}(t_{\alpha}),$$

where  $t_{\alpha} = \Phi_{\mathbb{Z}}^{-1}(1 - \alpha)$  and  $c_{\alpha} = \frac{\alpha + \Phi_{\mathbb{Z}}(t_{\alpha}) - 1}{\varphi(t)}$ . Then, it holds

$$\begin{aligned} \beta(\alpha) &= \mathbb{P}[X \leq t_{\alpha} - \mu] - c_{\alpha}\varphi_{\mathbb{Z}}(t_{\alpha} - \mu) \\ &= \Phi_{\mathbb{Z}}(\Phi_{\mathbb{Z}}^{-1}(1 - \alpha) - \mu) - \frac{\varphi_{\mathbb{Z}}(t_{\alpha} - \mu)}{\varphi_{\mathbb{Z}}(t_{\alpha})} (\alpha + \Phi_{\mathbb{Z}}(t_{\alpha}) - 1). \end{aligned}$$

□

By converting  $f$ -DP to  $(\epsilon, \delta)$ -DP using Proposition 2.12 in [Dong et al. \(2022\)](#) and Theorem A.7, we obtain that  $\widetilde{M}(D)$  is  $(\epsilon, \delta)$ -DP with

$$\delta(\epsilon) = \mathbb{P}\left[X > \frac{\epsilon\sigma^2}{\mu} - \frac{\mu}{2}\right] - e^{\epsilon}\mathbb{P}\left[X > \frac{\epsilon\sigma^2}{\mu} + \frac{\mu}{2}\right],$$

where the probability is taken with respect to  $X \sim \mathcal{N}_{\mathbb{Z}}(0, \sigma^2)$ . A similar result appears in Theorem 7 of [Canonne et al. \(2020\)](#). In practical applications, estimating the privacy profile for census data remains challenging due to the effects of composition, as illustrated in Figure 1a.

Mathematically, an  $n$ -fold composition of the DGM is represented by the sequence  $(\widetilde{M}_i(D))_{i=1}^n$ , where the associated hypothesis testing problem is given by:

$$H_0 : \left(\widetilde{M}_i(D)\right)_{i=1}^n \quad \text{vs.} \quad H_1 : \left(\widetilde{M}_i(D')\right)_{i=1}^n.$$

Here each  $\widetilde{M}_i(D) = M_i(D) + \mathcal{N}_{\mathbb{Z}}(0, \sigma_i^2)$ , with  $\sigma_i^2$  being a variance proxy of  $\mathcal{N}_{\mathbb{Z}}(0, \sigma_i^2)$  and  $M_i$  a given query. The  $f$ -DP guarantee corresponds to the hypothesis test:

$$H_0 : \prod_{i=1}^n P_i \quad \text{vs.} \quad H_1 : \prod_{i=1}^n Q_i,$$

where  $P_i$  is the distribution of  $\mathcal{N}_{\mathbb{Z}}(0, \sigma_i^2)$  and  $Q_i$  is that of  $\mathcal{N}_{\mathbb{Z}}(\mu_i, \sigma_i^2)$ , with  $\mu_i$  being the sensitivity of  $M_i$ . For i.i.d. noise with  $\mu_i \equiv \mu$  and  $\sigma_i \equiv \sigma$ , the  $f$ -DP guarantee is given in the following theorem.

**Theorem A.8.** For the hypothesis testing problem

$$H_0 : \mathcal{N}_{\mathbb{Z}}(0, \sigma^2) \times \mathcal{N}_{\mathbb{Z}}(0, \sigma^2) \text{ v.s. } H_1 : \mathcal{N}_{\mathbb{Z}}(\mu, \sigma^2) \times \mathcal{N}_{\mathbb{Z}}(\mu, \sigma^2)$$

with  $\mu \in \mathbb{Z}$ , we have the following closed-form representation of the type I and type II errors of the likelihood ratio test. The trade-off function is piecewise linear, where each knot has the form

$$\alpha(t) = \frac{c_{0, \sqrt{2}\sigma}}{c_{0, \sigma}^2} \left( \sum_{i > t/2, i \in \mathbb{Z}} e^{-i^2/\sigma^2} \right) + \frac{c_{-1/2, \sqrt{2}\sigma}}{c_{0, \sigma}^2} \left( \sum_{i > \frac{t-1}{2}, i \in \mathbb{Z}} e^{-(i+1/2)^2/\sigma^2} \right),$$

and the corresponding type II error is given by

$$\beta(t) = \frac{c_{0,\sqrt{2}\sigma}}{c_{0,\sigma}^2} \left( \sum_{i \leq t/2 - \mu} e^{-i^2/\sigma^2} \right) + \frac{c_{-1/2,\sqrt{2}\sigma}}{c_{0,\sigma}^2} \left( \sum_{i \leq \frac{t-1}{2} - \mu} e^{-(i+1/2)^2/\sigma^2} \right).$$

As a result, the 2-fold composition of the DGM is  $(\epsilon, \delta)$ -DP with

$$\delta(\epsilon) = 1 + \max_t \{-e^\epsilon \alpha(t) - \beta(t)\}.$$

**Remark.** The obtained Type I and Type II errors, as well as the privacy profile, are tight. According to Theorem A.8, to precisely specify the trade-off function, we need to partition the support of  $X_1 + X_2$  into two segments—  $(2\mathbb{Z}$  and  $2\mathbb{Z} + 1)$ . Each segment is associated with a coefficient,  $c_{0,\sqrt{2}\sigma}$  or  $c_{-1/2,\sqrt{2}\sigma}$ , and corresponds to a Gaussian distribution over the lattices  $2\mathbb{Z}$  or  $2\mathbb{Z} + 1$ . However, the resulting tight Type I and Type II errors are complex, involving the constants  $c_{0,\sqrt{2}\sigma}$  and  $c_{-1/2,\sqrt{2}\sigma}$ . It is noteworthy that  $c_{0,\sqrt{2}\sigma} \neq c_{-\frac{1}{2},\sqrt{2}\sigma}$ , differing from what is stated in Fact 18 of Canonne et al. (2020). For a correction to Fact 18 in Canonne et al. (2020), please refer to Proposition A.5. When  $\sigma$  is large, the difference between  $c_{0,\sqrt{2}\sigma}$  and  $c_{-1/2,\sqrt{2}\sigma}$  is negligible, which motivates our approximation of the  $n$ -fold composition of the DGM using a distribution supported on  $\mathbb{Z}/(\sqrt{n}\sigma)$  in Section A.4. In fact, if we replace  $c_{-1/2,\sqrt{2}\sigma}$  by  $c_{0,\sqrt{2}\sigma}$ , then the type I error can be approximated by

$$\frac{c_{0,\sqrt{2}\sigma}}{c_{0,\sigma}^2} \sum_{y > t, y \in \mathbb{Z}} \phi\left(\frac{y}{\sqrt{2}\sigma}\right),$$

where  $\phi$  is the pdf of the standard Gaussian distribution. Thus, we approximate the distribution of  $(X_1 + X_2)/(\sqrt{2}\sigma)$  by a measure  $\nu$  supported on  $\mathbb{Z}/\sqrt{2}\sigma$  (not a probability measure) with  $\nu[Y = i/\sqrt{2}\sigma] = \frac{1}{\sqrt{2}\sigma} \phi(i/\sqrt{2}\sigma)$  for some measurable function  $Y \sim \nu$ .

We can extend Theorem A.8 to i.i.d.  $n$ -fold composition. In fact, for  $n \geq 2$ , we have each knot of the type I error is

$$\alpha(t) = \mathbb{P} \left[ \sum_i X_i > t \right] = \sum_{k=0}^{n-1} c_{n,k} \sum_{y \in n\mathbb{Z}+k, y > t} e^{-\frac{y^2}{2\sigma^2}}, \quad (\text{A.5})$$

and the type II error is

$$\beta(t) = \mathbb{P} \left[ \sum_i X_i \leq t - n\mu \right] = \sum_{k=0}^{n-1} c_{n,k} \sum_{\substack{y \in n\mathbb{Z}+k, \\ y \leq t - n\mu}} e^{-\frac{y^2}{2\sigma^2}}, \quad (\text{A.6})$$

where  $c_{n,k} = e^{-\frac{k(n-1)}{2n\sigma^2}} \cdot \sum_{u_i \in \mathbb{Z}} e^{-\frac{\sum_{i=1}^n u_i^2 + 2\sum_{i=1}^k u_i + (\sum_{i=1}^{n-1} u_i)^2}{2\sigma^2}}$  is a finite constant.

Equation (A.5) and (A.6) reveal the structure underlying the summation of discrete Gaussian random variables. Specifically, the support  $\mathbb{Z}$  of  $\sum_i X_i$  is partitioned into  $n$  segments, with each segment corresponding to a Gaussian distribution over lattices. Each segment is associated with a distinct coefficient  $c_{n,k}$ , reflecting the distribution's structure across these lattice-based partitions.

Note that  $c_{n,k}$  is summing a discrete function across lattices of  $(n-1)$  dimensions. Computing this constant  $c_{n,k}$  is complicated, consequently complicating the practical application of the closed-form expressions found in Equations (A.5) and (A.6). To address this challenge, an efficient approximation method is introduced in Section A.4. Similar to the case  $n=2$ , in Section A.4, we approximate the distribution of  $\sum_{i=1}^n X_i/\sqrt{n}\sigma$  using a univariate random function  $Y \sim \nu$  with  $\nu[Y = i/\sqrt{n}\sigma] = \frac{1}{\sqrt{n}\sigma}\phi(i/\sqrt{n}\sigma)$ .

The independent but not identically distributed (i.n.i.d.) case, where  $X_1 \sim \mathcal{N}(0, \sigma_1^2)$  and  $X_2 \sim \mathcal{N}(0, \sigma_2^2)$ , is much more complicated. In fact, for  $n=2$ , the corresponding type I error becomes

$$\alpha(t) = \mathbb{P}[\sigma_2^2 X_1 + \sigma_1^2 X_2 > t].$$

The support of  $\sigma_2^2 X_1 + \sigma_1^2 X_2$  can be estimated only when  $\sigma_1^2, \sigma_2^2 \in a\mathbb{Z}$  for some  $a \in \mathbb{R}$  as a result of the Chinese remainder theorem. For simplicity, we consider  $a=1$  and the support of  $\sigma_2^2 X_1 + \sigma_1^2 X_2$  is  $\gcd(\sigma_1^2, \sigma_2^2) \times \mathbb{Z}$  according to the Chinese remainder theorem. For this i.n.i.d. case, the approximation of the privacy profile is derived in Section A.6.

#### A.4 Approximate the privacy profiles of discrete Gaussian mechanisms

To convert  $f$ -DP to  $(\epsilon, \delta)$ -DP, we adopt Proposition 3.2 in Wang et al. (2022). Let  $X_i \sim \mathcal{N}_{\mathbb{Z}}(0, \sigma_i^2)$  and  $Y_i \sim \mathcal{N}_{\mathbb{Z}}(\mu_i, \sigma_i^2)$ . Define  $\xi_i = \log \frac{q(Y_i)}{p(Y_i)}$  and  $\zeta_i = \log \frac{q(X_i)}{p(X_i)}$  with  $p$  and  $q$  being the probability density function of  $P$  and  $Q$ , respectively.

**Lemma A.9** (Proposition 3.2 in Wang et al. (2022)). The  $n$ -fold composition of the DGM  $(\widetilde{M}_i(D))_{i=1}^n$  is  $(\epsilon, \delta)$ -DP with

$$\delta(\epsilon) = \mathbb{P}\left[\sum_{i=1}^n \xi_i > \epsilon\right] - e^\epsilon \mathbb{P}\left[\sum_{i=1}^n \zeta_i > \epsilon\right].$$

For the i.i.d. case where  $\sigma_i \equiv \sigma$ , we obtain the following privacy profile for the  $n$ -fold composition of the DGM.

**Proposition A.10** (Privacy profile for the i.i.d. composition of the DGM). For the i.i.d. case with  $\sigma_i \equiv \sigma$ , the  $n$ -fold composition of the DGM  $(\widetilde{M}_i(D))_{i=1}^n$  is  $(\epsilon, \delta)$ -DP with

$$\delta(\epsilon) = \mathbb{P}\left[S_n > \frac{1}{B_n} \left(\frac{2\epsilon\sigma^2}{2} - \frac{n}{2}\right)\right] - e^\epsilon \mathbb{P}\left[S_n > \frac{1}{B_n} \left(\frac{2\epsilon\sigma^2}{2} + \frac{n}{2}\right)\right],$$

where  $S_n = \frac{1}{B_n} \sum_{i=1}^n X_i$ ,  $B_n = \sqrt{n}\sigma$ .

Proposition A.10 is a straightforward conclusion of Lemma A.9 and Equation (A.5). Note that the support is scaled to  $\mathbb{Z}/B_n$  and we approximate the composition by the following 1-dimensional distribution over lattices  $\mathbb{Z}/B_n$ .

**Theorem A.11.** Consider  $M(D) = (M_i(D))_{i=1}^n$  with  $M_i(D) \in \mathbb{R}$  being a counting query with sensitivity 1. Let  $\widetilde{M}_i(D) = M_i(D) + \mathcal{N}_{\mathbb{Z}}(0, \sigma^2)$  for any  $\sigma^2 \in \mathbb{R}$ . Then, we have  $\widetilde{M}(D) = (\widetilde{M}_i(D))_{i=1}^n$  is  $(\epsilon, \delta)$ -DP with

$$\delta(\epsilon) = \frac{1}{B_n} \sum_{\substack{U_1 \\ \frac{i}{B_n} > \frac{2\sigma^2\epsilon - n}{2B_n}}} \phi\left(\frac{i}{B_n}\right) - e^\epsilon \left( \frac{1}{B_n} \sum_{\substack{U_2 \\ \frac{i}{B_n} > \frac{2\sigma^2\epsilon + n}{2B_n}}} \phi\left(\frac{i}{B_n}\right) + R_2(n, \sigma, \epsilon) \right) + R_1(n, \sigma, \epsilon),$$

where  $U_1 = \max\{20, \frac{2\sigma^2\epsilon-n}{2B_n}\}$  and  $U_2 = \max\{20, \frac{2\sigma^2\epsilon+n}{2B_n}\}$ .  $R_1(n, \sigma, \epsilon)$  and  $R_2(n, \sigma, \epsilon)$  are residual terms computed by the Fourier transform with

$$R_1(n, \sigma, \epsilon) \leq \sum_{\substack{U_1 \\ \frac{i}{B_n} > \frac{2\sigma^2\epsilon-n}{2B_n}}} r_{n,\sigma} \left( \frac{i}{B_n} \right) + \mathbb{P}[S_n > U_1], \quad \text{and}$$

$$R_2(n, \sigma, \epsilon) \leq \sum_{\substack{U_2 \\ \frac{i}{B_n} > \frac{2\sigma^2\epsilon+n}{2B_n}}} r_{n,\sigma} \left( \frac{i}{B_n} \right) + \mathbb{P}[S_n > U_2].$$

Here,  $r_{n,\sigma}$  has a closed-form representation

$$r_{n,\sigma}(y) = \frac{1}{2\pi B_n} \left| \int_{-\pi B_n}^{\pi B_n} e^{-t^2/2} e^{-ity} \left( \frac{\theta_3 \left( -i\sigma\pi t / \sqrt{n}, e^{-2\sigma^2\pi^2} \right)}{\theta_3 \left( 0, e^{-2\sigma^2\pi^2} \right)} \right)^n dt - \int_{-\infty}^{\infty} e^{-t^2/2} e^{-ity} dt \right|,$$

with  $\theta_3(u, q) = 1 + 2 \sum_{k=1}^{\infty} q^{k^2} \cos(2ku)$  being a theta function.

In Theorem A.11, we approximate the probability mass function of  $S_n$  using a function (not a probability mass function)  $\frac{1}{B_n} \phi \left( \frac{i}{B_n} \right)$ . The error associated with this approximation is examined in detail in Section A.5. For the case  $n = 2$ , where the pmf of  $S_n$  can be computed directly, we compare  $\frac{1}{B_n} \phi \left( \frac{i}{B_n} \right)$  with the actual pmf of  $S_n$  in Figure 6. From Figure 6, we observe that our approximation should be powerful intuitively. We provide a numerical estimate of the residuals  $R_1(n, \sigma, \epsilon)$  and  $R_2(n, \sigma, \epsilon)$  in Section A.5. Approximating the  $n$ -fold composition using a 1-dimension distribution is also investigated by Genise et al. (2020); Kairouz et al. (2021), where they approximate the  $n$ -dimensional discrete Gaussian distribution using  $W_n \sim \mathcal{N}_{\mathbb{Z}}(0, n\sigma^2)$ . Moreover, an analytical upper bound on the approximation error is given in Corollary 12 of Kairouz et al. (2021).

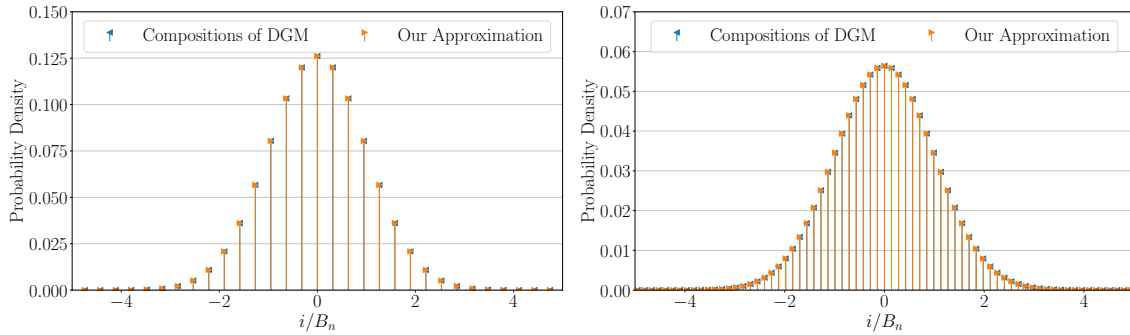


Figure 6: Comparisons of pmf and approximation with  $\sigma^2 = 5$  (left) and  $\sigma^2 = 25$  (right).

*Proof of Theorem A.11.* According to Lemma A.9 and Proposition A.10, we have, for any  $y \in \mathbb{Z}/B_n$ ,

$$r_{n,\sigma}(y) = \mathbb{P}[S_n = y] - \frac{1}{B_n} \phi(y).$$



For  $\phi(y)$ , we have the following Fourier inversion formula:

$$\phi(y) = \frac{1}{2\pi} \int_{-\infty}^{\infty} e^{-t^2/2} e^{-ity} dt.$$

Using the inversion formula for discrete distribution (cf., Exercise 3.3.2 (iii) in Durrett (2019)), we have

$$\mathbb{P}[S_n = y] = \frac{1}{2\pi B_n} \int_{-\pi B_n}^{\pi B_n} e^{-i\zeta y} f_{S_n}(\zeta) d\zeta,$$

where  $f_{S_n}$  is the characteristic function of  $S_n$ , i.e.,  $f_{S_n}(y) = \mathbb{E}_{S_n} e^{iyS_n}$ . Equation (A.3) shows that,

$$f_{S_n}(t) = \mathbb{E} e^{itS_n} = e^{-t^2/2} \left( \frac{\theta_3\left(-i\sigma\pi t/\sqrt{n}, e^{-2\sigma^2\pi^2}\right)}{\theta_3\left(0, e^{-2\sigma^2\pi^2}\right)} \right)^n.$$

This completes the proof of Theorem A.11. □

## A.5 Estimate the residual

This subsection is to numerically estimate the residual terms  $R_1(n, \sigma, \epsilon)$  and  $R_2(n, \sigma, \epsilon)$  in Theorem A.11. Technical details are deferred to Section C.

Numerically, we found that the residual term can indeed be extremely small for applications such as the Census. To estimate the residual term  $R_1(n, \sigma, \epsilon)$ , we decompose it as follows:

$$R_1(n, \sigma, \epsilon) = \sum_{\substack{U_1 \\ \frac{i}{B_n} > \frac{2\sigma^2\epsilon - n}{2B_n}}} r_{n,\sigma} \left( \frac{i}{B_n} \right) + \mathbb{P}[S_n > U_1] =: \mathcal{E}_{11} + \mathcal{E}_{12}.$$

For the error term  $\mathcal{E}_{11}$ , we note that  $r_{n,\sigma}$  achieves an extremely small error that makes  $\mathcal{E}_{11}$  negligible. We have listed the estimates of  $r_{n,\sigma}(i/B_n)$  in Table 2 which hold uniformly for all  $i \in \mathbb{Z}$ . In the applications of the Census 2020, where  $n$  is at least 10 and the smallest  $\sigma^2$  is 4.99, an error of  $3.0 \times 10^{-37}$  is insignificant compared to the bureau's choice of  $\delta = 10^{-10}$ . The details of the numerical bounds can be found in Section C.

For the second error term  $\mathcal{E}_{12}$ , we bound it using the sub-Gaussian tail bound (A.2) and obtain

$$\mathcal{E}_{12} = \mathbb{P}[S_n > U_1] \leq e^{-20^2/2}.$$

Note that this term is numerically smaller than  $1.4 \times 10^{-87}$ .

The other error term  $R_2(n, \sigma, \epsilon)$  can be estimated similarly as follows:

$$R_2(n, \sigma, \epsilon) = \sum_{\substack{U_2 \\ \frac{i}{B_n} > \frac{2\sigma^2\epsilon + n}{2B_n}}} r_{n,\sigma} \left( \frac{i}{B_n} \right) + \mathbb{P}[S_n > U_2] =: \mathcal{E}_{21} + \mathcal{E}_{22}.$$

The two terms  $\mathcal{E}_{21}$  and  $\mathcal{E}_{22}$  can be estimated similarly. Precisely,  $\mathcal{E}_{22}$  is bounded using the sub-Gaussian tail bound and  $\mathcal{E}_{21}$  is bounded using Table 2. Then, the overall privacy budget is counted

Estimate of the residual $r_{n,\sigma}$				
$n$ -fold Compositions of $\mathcal{N}_{\mathbb{Z}}(0, \sigma^2)$	$\sigma^2 = 1$	$\sigma^2 = 5$	$\sigma^2 = 10$	$\sigma^2 \geq 16$
$n = 5$	$5 \times 10^{-6}$	$3 \times 10^{-32}$	$2 \times 10^{-65}$	$\ll 10^{-100}$
$n = 9$	$5 \times 10^{-7}$	$1 \times 10^{-36}$	$4 \times 10^{-74}$	$\ll 10^{-100}$
$n = 10$	$4 \times 10^{-7}$	$3 \times 10^{-37}$	$3 \times 10^{-75}$	$\ll 10^{-100}$
$n = 18$	$2 \times 10^{-7}$	$2 \times 10^{-39}$	$2 \times 10^{-79}$	$\ll 10^{-100}$
$n = 20$	$9 \times 10^{-8}$	$8 \times 10^{-40}$	$4 \times 10^{-80}$	$\ll 10^{-100}$
$n = 27$	$7 \times 10^{-8}$	$2 \times 10^{-40}$	$2 \times 10^{-81}$	$\ll 10^{-100}$
$n = 50$	$4 \times 10^{-8}$	$2 \times 10^{-41}$	$3 \times 10^{-83}$	$\ll 10^{-100}$
$n = 100$	$2 \times 10^{-8}$	$6 \times 10^{-42}$	$3 \times 10^{-84}$	$\ll 10^{-100}$

Table 2: We bound the residual term  $\sup_{y \in \mathbb{Z}/B_n} r_{n,\sigma}(y)$  numerically.

as

$$\left| \delta(\epsilon) - \left\{ \frac{1}{B_n} \sum_{\substack{i > \frac{2\sigma^2\epsilon - n}{2B_n} \\ i < \frac{2\sigma^2\epsilon + n}{2B_n}} \phi\left(\frac{i}{B_n}\right) - e^\epsilon \left( \frac{1}{B_n} \sum_{\substack{i > \frac{2\sigma^2\epsilon - n}{2B_n} \\ i < \frac{2\sigma^2\epsilon + n}{2B_n}} \phi\left(\frac{i}{B_n}\right) \right) \right\} \right| \leq \mathcal{E}_{11} + \mathcal{E}_{12} + e^\epsilon (\mathcal{E}_{21} + \mathcal{E}_{22}). \quad (\text{A.7})$$

Based on the upper bound in (A.7) and the error estimate in Table 2, we obtain the privacy budget  $\epsilon$  in Figure 2 by solving  $\delta(\epsilon) = 10^{-11}$  using binary search. In addition to the number of folds of the composition in Table 2, Figure 7 compares our method using the ACS 5-year estimates with  $n = 1890$ . It shows that our method enjoys greater advantage when the number of folds under composition is larger.

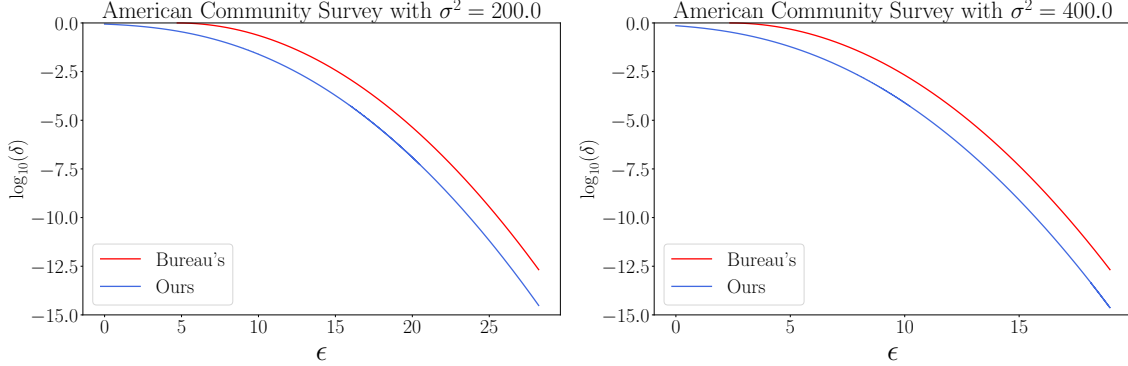


Figure 7: Comparisons with zCDP using American Community Survey 5-year data, a smaller  $(\epsilon, \delta)$ -curve means the privatized dataset is more private.

## A.6 Counting the overall privacy budget of Allocation 2022-08-25

This section is to count the overall privacy budget among all 8 geographical levels that corresponds to total heterogeneous composition of the DGMs, which contains independent but not identically

distributed (i.n.i.d.) discrete Gaussian noise for different geographical levels. The technical details of all this section is postponed to Section D.

$a_1$	$a_2$	$a_3$	$a_4$	$a_5$	$a_6$	$a_7$
2.0%	27.40%	8.50%	13.10%	23.80%	11.80%	0.3%
$n_1$	$n_2$	$n_3$	$n_4$	$n_5$	$n_6$	$n_7$
10	10	10	20	10	10	10

Table 3: Actual allocation of the  $a_i$  and number of folds of composition  $n_i$  for each geographical level in Privacy-loss Budget Allocation 2022-08-25 (US Census Bureau, 2022a).

The allocation adopted by the bureau (the row corresponding to Bureau's) in Table 1, is from the file released on 2022-08-25 (US Census Bureau, 2022a). To count the overall privacy budget of the Allocation 2022-08-25, we divide the the 80-fold i.n.i.d. composition into  $k$  groups and each group  $i$  is  $n_i$ -fold i.i.d. composition with  $n_i$  being given in Table 3. Let  $\rho = 3.65$  be the total  $\rho$ -zCDP budget in Privacy-loss Budget Allocation 2022-08-25 and let  $a_i$  be the allocation of the budget  $\rho$  in the  $i$ -th geographical level. Moreover, denote  $n = 10$ , for each geographical level, each query is added an i.i.d.  $\mathcal{N}_{\mathbb{Z}}(0, \sigma_i^2)$  with  $\sigma_i^2 = \frac{n}{2a_i\rho}$ . Then, the privacy profile is

$$\begin{aligned} \delta(\epsilon) &= \mathbb{P}_{X_{ij} \sim \mathcal{N}_{\mathbb{Z}}(0, \sigma_i^2)} \left[ \sum_{i=1}^k \frac{1}{\sigma_i^2} \sum_{j=1}^{n_i} X_{ij} > \epsilon - \sum_{i=1}^k \sum_{j=1}^{n_i} \frac{1}{2\sigma_i^2} \right] \\ &\quad - e^\epsilon \cdot \mathbb{P}_{X_{ij} \sim \mathcal{N}_{\mathbb{Z}}(0, \sigma_i^2)} \left[ \sum_{i=1}^k \frac{1}{\sigma_i^2} \sum_{j=1}^{n_i} X_{ij} > \epsilon + \sum_{i=1}^k \sum_{j=1}^{n_i} \frac{1}{2\sigma_i^2} \right], \end{aligned} \tag{A.8}$$

which is further simplified to

$$\begin{aligned} \delta(\epsilon) &= \mathbb{P}_{X_{ij} \sim \mathcal{N}_{\mathbb{Z}}(0, \sigma_i^2)} \left[ \sum_{i=1}^k a_i \sum_{j=1}^{n_i} X_{ij} > \epsilon \cdot \frac{n}{2\rho} - \sum_{i=1}^k \sum_{j=1}^{n_i} \frac{a_i}{2} \right] \\ &\quad - e^\epsilon \cdot \mathbb{P}_{X_{ij} \sim \mathcal{N}_{\mathbb{Z}}(0, \sigma_i^2)} \left[ \sum_{i=1}^k a_i \sum_{j=1}^{n_i} X_{ij} > \epsilon \cdot \frac{n}{2\rho} + \sum_{i=1}^k \sum_{j=1}^{n_i} \frac{a_i}{2} \right] \\ &= \mathbb{P}_{X_{ij} \sim \mathcal{N}_{\mathbb{Z}}(0, \sigma_i^2)} \left[ \sum_{i=1}^k a_i \sum_{j=1}^{n_i} X_{ij} > \epsilon \cdot \frac{n}{2\rho} - \frac{n}{2} \right] \\ &\quad - e^\epsilon \cdot \mathbb{P}_{X_{ij} \sim \mathcal{N}_{\mathbb{Z}}(0, \sigma_i^2)} \left[ \sum_{i=1}^k a_i \sum_{j=1}^{n_i} X_{ij} > \epsilon \cdot \frac{n}{2\rho} + \frac{n}{2} \right], \end{aligned}$$

where the last equality follows from the fact that  $\sum_{i=1}^k \sum_{j=1}^{n_i} a_i = n$ .

**Outline of our approximation of the privacy profile.** Let  $t_\epsilon = \frac{n}{2} \left( \frac{\epsilon}{\rho} - 1 \right)$ , to make our estimate of the privacy profile  $\delta(\epsilon)$  easier to understand, we summarize our pipeline as follows.

$$\begin{aligned} & \mathbb{P}_{X_{ij} \sim \mathcal{N}_{\mathbb{Z}}(0, \sigma_i^2)} \left[ \sum_{i=1}^k a_i \sum_{j=1}^{n_i} X_{ij} > t_\epsilon \right] \stackrel{\text{Prop. A.12}}{\approx} \nu \left( \sum_{i=1}^k a_i \bar{X}_i \geq t_\epsilon \right) \\ & \stackrel{\text{Prop. A.13}}{\approx} \int_0^\pi F(t) dt \stackrel{\text{Fact A.14}}{\approx} \int_0^{\frac{1}{100}} F(t) dt \\ & \stackrel{\text{Fact A.15}}{\approx} \sum_{k=1}^{\frac{10^7}{4}} \frac{2}{100 \times 45 \times 10^7} \times (7 * F(x_{4k-4}) + 32F(x_{4k-3}) + 12F(x_{4k-2}) + 32F(x_{4k-1}) + 7F(x_{4k})), \end{aligned}$$

with some measure  $\nu$  and function  $F(t)$  defined later in Proposition A.12 and A.13, respectively. The errors in all the approximate equalities above can be bounded numerically, and we will demonstrate that these errors are small. Additionally, the final approximation comes from the Boole sum, which is also computable numerically. As a result, the privacy profile can be efficiently computed.

### Details of our approximation of the privacy profile.

**Proposition A.12.** We have

$$\left| \mathbb{P}_{X_{ij} \sim \mathcal{N}_{\mathbb{Z}}(0, \sigma_i^2)} \left[ \sum_{i=1}^k a_i \sum_{j=1}^{n_i} X_{ij} > t_\epsilon \right] - \nu \left( \sum_{i=1}^k a_i \bar{X}_i \geq t_\epsilon \right) \right| < \mathcal{E}_0^{(0)} + \mathcal{E}_1^{(0)} + \mathcal{E}_2^{(0)},$$

where  $\mathcal{E}_i^{(0)}$ , for  $i \leq 3$ , are constants satisfying the following conditions:

$$\begin{aligned} \mathcal{E}_0^{(0)} &= k \times e^{-12^2/2}, \\ \mathcal{E}_1^{(0)} &= k \times e^{-12^2/2}, \end{aligned}$$

$$\mathcal{E}_2^{(0)} = \prod_{i=1}^k (24\sqrt{n_i}\sigma_i) \cdot \sum_{i=1}^k r_{n_i, \sigma_i} \cdot \max_{\{y_j\}_{j=1}^k \in \mathbb{Z}^k} \left| \left( \prod_{j=1}^{i-1} c_j \right) \left( \prod_{j=i+1}^k b_j \right) \right|,$$

with

$$c_i = \mathbb{P}_{X_{ij} \sim \mathcal{N}_{\mathbb{Z}}(0, \sigma_i^2)} \left[ \sum_{j=1}^{n_i} X_{ij} = y_i \right] \leq \frac{1}{\sqrt{n_i \sigma_i^2}} \phi \left( \frac{y_i}{\sqrt{n_i \sigma_i^2}} \right) + r_{n_i, \sigma_i} \leq \frac{1}{\sqrt{2\pi n_i \sigma_i^2}} + r_{n_i, \sigma_i},$$

and

$$b_i = \frac{1}{\sqrt{n_i \sigma_i^2}} \phi \left( \frac{y_i}{\sqrt{n_i \sigma_i^2}} \right) \leq \frac{1}{\sqrt{2\pi n_i \sigma_i^2}},$$

and  $\{\bar{X}_i\}_{1 \leq i \leq k}$  is a sequence of independent discrete measurable functions on  $\mathbb{Z}$ , with measure (not a probability measure)

$$\nu(\bar{X}_i = \mathbf{x}) = \frac{1}{\sqrt{n_i \sigma_i^2}} \phi \left( \frac{x}{\sqrt{n_i \sigma_i^2}} \right),$$

for  $\mathbf{x} \in \mathbb{Z}$ .

**Upper bound on  $\mathcal{E}_i^{(0)}$ .** According to Table 2, numerically, we have

$$\mathcal{E}_2^{(0)} = \prod_{i=1}^k (24\sqrt{n_i}\sigma_i) \cdot \sum_{i=1}^k r_{n_i, \sigma_i} \cdot \max_{\{y_j\}_{j=1}^k \in \mathbb{Z}^k} \left| \left( \prod_{j=1}^{i-1} c_j \right) \left( \prod_{j=i+1}^k b_j \right) \right| \leq 3.4 \times 10^{-29}.$$

Since  $e^{(-12^2/2)} < 5.4 \times 10^{-32}$ , overall, we have

$$\mathcal{E}_0^{(0)} + \mathcal{E}_1^{(0)} + \mathcal{E}_2^{(0)} < 3.4 \times 10^{-29} + 7 \times 5.4 \times 10^{-32} + 7 \times 5.4 \times 10^{-32} < 3.41 \times 10^{-29}.$$

**Proposition A.13.** The following approximation to  $\nu$  holds.

$$\left| \nu \left( \sum_{i=1}^k a_i \bar{X}_i \geq t_\epsilon \right) - \int_0^\pi F(t) dt \right| < \mathcal{E}^{(1)}, \quad (\text{A.9})$$

where

$$F(t) = \frac{1}{2\pi} \left[ \cos(\lceil t_\epsilon L \rceil \cdot t) + \cos(\lceil 6t_\epsilon L \rceil \cdot t) + \frac{\cos(t/2)}{\sin(t/2)} (\sin(\lceil 6t_\epsilon L \rceil \cdot t) - \sin(\lceil t_\epsilon L \rceil \cdot t)) \right] \prod_{i=1}^k f_{\bar{X}_i}(a_i Lt),$$

$$\mathcal{E}^{(1)} = \nu \left( \bar{X}_i > \frac{6 \times t_\epsilon L}{k \cdot L \cdot a_i} \right), \text{ for } L = 10^3 \text{ and } a_i \text{ given in Table 3.}$$

Moreover, the characteristic function  $f_{\bar{X}_i}(a_i Lt)$  is given by

$$f_{\bar{X}_i}(a_i Lt) = \frac{1}{\sqrt{2\pi n_i \sigma_i^2}} + 2 \sum_{u=1}^{\infty} \cos(ua_i Lt) \cdot \frac{e^{-\frac{u^2}{2} \cdot \frac{1}{n_i \sigma_i^2}}}{\sqrt{2\pi n_i \sigma_i^2}}.$$

A similar result holds by replacing  $t_\epsilon$  to  $T_\epsilon = \epsilon + \sum_{i=1}^k \sum_{j=1}^{n_i} \frac{1}{2\sigma_i^2}$ .

**Upper bound on  $\mathcal{E}^{(1)}$ .** Numerically, one can verify that  $\mathcal{E}^{(1)} \leq 5.6 \times 10^{-29}$ .

Although Equation (A.9) is very complicated, the following decomposition simplified the computation by further approximating (A.9). Precisely, the following fact indicates that we only need to consider the integral from 0 to  $\frac{1}{100}$ .

**Fact A.14.** The equation below shows that the integral of  $F(t)$  over the interval  $[0, \pi]$  is almost the same as the integral over  $[0, 1/100]$ :

$$\left| \int_0^\pi F(t) dt - \int_0^{\frac{1}{100}} F(t) dt \right| = \mathcal{E}^{(2)}, \quad (\text{A.10})$$

with  $\mathcal{E}^{(2)} \leq 1.3 \times 10^{-30}$ . The remaining portion of the integral  $\mathcal{E}^{(2)}$  beyond  $\frac{1}{100}$  is negligible.

Although Equation (A.10) simplified the integral, it is still complicated to numerically compute the integral. We have performed the numerical integral by using Mathematica, vpaintegration in Matlab and mpmath.quad in Python. Unfortunately, none of them give us the accurate answer when the error tolerance is  $10^{-30}$ . Therefore, we choose to manually compute the Boole's Sum of Equation (A.10).

**Fact A.15.** Recall the definition of  $F(t)$  from Proposition A.13. We numerically evaluate the integral of  $F(t)$  over the interval  $[0, 1/100]$  using Boole’s rule, employing a partition of  $N = 10^7 + 1$  points, denoted as  $\{x_i\}_{i=1}^N$ , where

$$x_i = i * h, \quad \text{with } h = \frac{1}{100(N - 1)},$$

for  $i = 0, \dots, N - 1$ . Then, the following approximation holds

$$\left| \int_0^{\frac{1}{100}} F(t) dt - \sum_{l=1}^{\frac{N-1}{4}} \frac{2h}{45} \times (7 * F(x_{4l-4}) + 32F(x_{4l-3}) + 12F(x_{4l-2}) + 32F(x_{4l-1}) + 7F(x_{4l})) \right| = \mathcal{E}^{(3)},$$

with  $\mathcal{E}^{(3)} \leq 2.54 \times 10^{-24}$ .

**Total approximation error.** Overall, we can approximate the first term of the privacy profile  $\delta(\epsilon), \mathbb{P}_{X_{ij} \sim \mathcal{N}_{\mathbb{Z}}(0, \sigma_i^2)} \left[ \sum_{i=1}^k a_i \sum_{j=1}^{n_i} X_{ij} > t_\epsilon \right]$ , by using the sum:

$$\sum_{k=1}^{\frac{N-1}{4}} \frac{2h}{45} \times (7 * F(x_{4k-4}) + 32F(x_{4k-3}) + 12F(x_{4k-2}) + 32F(x_{4k-1}) + 7F(x_{4k})).$$

This can be efficiently computed with numerical methods. The total approximation error is bounded by  $\mathcal{E}_0^{(0)} + \mathcal{E}_1^{(0)} + \mathcal{E}_2^{(0)} + \mathcal{E}^{(1)} + \mathcal{E}^{(2)} + \mathcal{E}^{(3)} < 2.6 \times 10^{-24}$ .

**Computation time.** Computing the privacy budget  $(\epsilon, \delta(\epsilon))$  within each geographical level as in Figure 2 takes less than 5 minute. However, calculating the overall privacy budget as in Section A.6 across all eight levels requires more time. For each  $\epsilon$ ,  $\delta(\epsilon)$  can be computed within 9.5 hours using an AWS EC2 c5.metal instance with 96×2GB virtual CPUs.

Accounting for privacy budgets using characteristic functions has been widely employed in previous literature, Koskela et al. (2020); Gopi et al. (2021); Zhu et al. (2022). However, the computation time of our approach significantly outperforms previous methods. To attain an error below  $10^{-12}$ , prior methods relied on the Riemann sum for numerical integral, resulting in a computational cost of at least  $O(N)$  with  $N = 3.4 \times 10^{16}$ , which is computationally infeasible. In contrast, our approach in Proposition A.13 and Fact A.15 leverages Boole’s sum rather than the Riemann sum to calculate the Fourier transform, resulting in a significant improvement in computational efficiency. Additionally, Equation (A.10) enhances computation by splitting the integral into a main body and a remainder, with the remainder bounded by  $1.3 \times 10^{-30}$ . Consequently, only the main part of the integral needs to be computed. Overall, this results in a computational cost of  $O(N)$  with  $N = 10^7$ .

**Limitations in the computations.** We would like to briefly discuss the primary limitation encountered in the numerical computations. Recall the privacy profile defined in Equation (A.8). The parameter  $\delta$  used in the Privacy-loss Budget Allocation released on August 25, 2022, is set to  $10^{-10}$ , which imposes a requirement that the second probability in Equation (A.8) be less than  $10^{-10}/e^{21.97} \approx 2.8 \times 10^{-20}$ . This value is smaller than the precision limit of Python’s floating-point

arithmetic. Consequently, it is extremely difficult to compute this term numerically, even with high-precision libraries such as `mpmath` or `scipy`. As a result, in Section 2.4, for any  $\epsilon$ , we present the following upper bound of the overall privacy budget  $\delta(\epsilon)$ :

$$\delta(\epsilon) < \mathbb{P}_{X_{ij} \sim \mathcal{N}_{\mathbb{Z}}(0, \sigma_i^2)} \left[ \sum_{i=1}^k \frac{1}{\sigma_i^2} \sum_{j=1}^{n_i} X_{ij} > \epsilon - \sum_{i=1}^k \sum_{j=1}^{n_i} \frac{1}{2\sigma_i^2} \right].$$

This limitation results in the overall privacy budget calculated in Section 2.4 showing less significant improvement compared to Figure 2.

## B Omitted details of Section A.2

### B.1 Proof of Lemma A.4

By the Poisson Summation Formula, we have

$$\sum_{x \in \mathbb{Z}} e^{-\frac{(x-\mu)^2}{2\sigma^2}} = \sqrt{2\pi\sigma^2} \sum_{x \in \mathbb{Z}} e^{-2\pi^2\sigma^2 x^2} e^{-2\pi i \mu x}.$$

According to the Jacobi triple product, for  $q = e^{-2\pi^2\sigma^2}$  and  $z = e^{-2\pi i \mu}$ , the following equality holds.

$$\sum_{x \in \mathbb{Z}} e^{-2\pi^2\sigma^2 x^2} e^{-2\pi i \mu x} = \prod_{m=0}^{\infty} (1 - q^{2m+2})(1 + zq^{2m+1})(1 + z^{-1}q^{2m+1}).$$

Therefore, one has

$$\begin{aligned} \frac{\sum_{x \in \mathbb{Z}} e^{-\frac{(x-\mu)^2}{2\sigma^2}}}{\sum_{x \in \mathbb{Z}} e^{-\frac{(x-\nu)^2}{2\sigma^2}}} &= \frac{\sum_{x \in \mathbb{Z}} e^{-2\pi^2\sigma^2 x^2} e^{-2\pi i \mu x}}{\sum_{x \in \mathbb{Z}} e^{-2\pi^2\sigma^2 x^2} e^{-2\pi i \nu x}} \\ &= \prod_{m=0}^{\infty} \frac{(1 + e^{-2\pi i \mu} q^{2m+1})(1 + e^{2\pi i \mu} q^{2m+1})}{(1 + e^{-2\pi i \nu} q^{2m+1})(1 + e^{2\pi i \nu} q^{2m+1})} \\ &= \prod_{m=0}^{\infty} \frac{1 + q^{4m+2} + 2 \cos(2\pi \mu) q^{2m+1}}{1 + q^{4m+2} + 2 \cos(2\pi \nu) q^{2m+1}}. \end{aligned}$$

Since  $q > 0$  and  $\cos(x)$  is an decreasing function in  $[0, \pi]$ , we have

$$\frac{\sum_{x \in \mathbb{Z}} e^{-\frac{(x-\mu)^2}{2\sigma^2}}}{\sum_{x \in \mathbb{Z}} e^{-\frac{(x-\nu)^2}{2\sigma^2}}} = \prod_{m=0}^{\infty} \frac{1 + q^{4m+2} + 2 \cos(2\pi \mu) q^{2m+1}}{1 + q^{4m+2} + 2 \cos(2\pi \nu) q^{2m+1}} > 1.$$

This completes the proof of this lemma.



## B.2 Proof of Proposition A.6

Recall Equation (A.3). It suffices to show that  $\sum_{u=-\infty}^{\infty} e^{-\sigma^2(t/B_n - 2\pi u)^2/2}$  is non-increasing with respect to  $t \in (0, \pi B_n)$ . To see this, consider the following derivative:

$$\begin{aligned} & \frac{d}{dt} \sum_{u=-\infty}^{\infty} e^{-\sigma^2(t/B_n - 2\pi u)^2/2} \\ &= \frac{d}{dt} \sum_{u=-\infty}^{\infty} e^{-(2\pi\sigma)^2(t/(2\pi B_n) - u)^2/2}. \end{aligned}$$

Let  $\mu$  and  $\sigma^2$  in Equation (A.4) be  $t/(2\pi B_n)$  and  $1/(2\pi\sigma)^2$ , respectively. Then, we have

$$\frac{d}{dt} \sum_{u \in \mathbb{Z}} e^{-\frac{(2\pi\sigma)^2(u - t/(2\pi B_n))^2}{2}} < 0,$$

for any  $0 < t/(2\pi B_n) < 1/2$ .

## C Omitted details of Section A.5

Recall that  $B_n = \sqrt{n\sigma^2}$ . The main ingredient is to characterize the distribution of  $S_n$  and bound the difference between the characteristic function of  $S_n$  and that of  $\frac{1}{B_n}\phi\left(\frac{i}{B_n}\right)$ . As the residual term is estimated numerically and the numerical error depends on both  $\sigma$  and  $n$ , for conciseness, we adopt the example  $\sigma^2 = 5$  and  $n = 10$  (the smallest  $n$  and  $\sigma$  in real allocation files that implies the largest numerical error in our method). The numerical estimate of the residual can be extended to any  $\sigma$  and  $n$ .

**Fact C.1** (Estimate the residual of  $N_{\mathbb{Z}}(0, 5)$  and  $n = 10$ ). For any  $x \in \mathbb{Z}$ , we have

$$\sup_{x \in \mathbb{Z}} r_{n,\sigma}\left(\frac{x}{B_n}\right) = \sup_{x \in \mathbb{Z}} \left| \mathbb{P}\left(S_n = \frac{x}{B_n}\right) - \frac{1}{B_n}\phi\left(\frac{x}{B_n}\right) \right| < 2.6 \times 10^{-37}.$$

### C.1 Calculation of Fact C.1

For any  $y \in \mathbb{Z}/B_n$ , recall the residual term

$$\begin{aligned} r_{n,\sigma}(y) &= \left| \mathbb{P}(S_n = y) - \frac{1}{B_n}\phi(y) \right| \\ &= \frac{1}{2\pi B_n} \left| \int_{-\pi B_n}^{\pi B_n} e^{-ity} f_{S_n}(t) dt - \int_{-\infty}^{\infty} e^{-t^2/2} e^{-ity} dt \right|, \end{aligned}$$

where  $f_{S_n}$  is the characteristic function of  $S_n$ . Recall the closed-form representation of  $f_{S_n}$  in (A.3), i.e.,

$$f_{S_n}(t) = \mathbb{E} e^{itS_n} = e^{-t^2/2} \left( \frac{\theta_3\left(-i\sigma\pi t/\sqrt{n}, e^{-2\sigma^2\pi^2}\right)}{\theta_3\left(0, e^{-2\sigma^2\pi^2}\right)} \right)^n.$$

Then, we have

$$\begin{aligned}
& \left| \mathbb{P}(S_n = y) - \frac{1}{B_n} \phi(y) \right| \\
& \leq \frac{1}{2\pi B_n} \left| \int_{-\pi B_n}^{\pi B_n} e^{-ity} f_{S_n}(t) dt - \int_{-\infty}^{\infty} e^{-t^2/2} e^{-ity} dt \right| \\
& \leq \frac{1}{2\pi B_n} \left| \int_{-\pi B_n}^{\pi B_n} e^{-ity} f_{S_n}(t) dt - \int_{-\pi B_n}^{\pi B_n} e^{-t^2/2} e^{-ity} dt \right| + \frac{1}{\pi B_n} \int_{\pi B_n}^{\infty} e^{-t^2/2} dt \\
& \leq \frac{1}{2\pi B_n} \int_{-\pi B_n}^{\pi B_n} |f_{S_n}(t) - e^{-t^2/2}| dt + \frac{1}{\pi B_n} \int_{\pi B_n}^{\infty} e^{-t^2/2} dt.
\end{aligned}$$

We decompose the upper bound into following parts:

$$\begin{aligned}
& \frac{1}{2\pi B_n} \int_{-\pi B_n}^{\pi B_n} |f_{S_n}(t) - e^{-t^2/2}| dt + \frac{1}{\pi B_n} \int_{\pi B_n}^{\infty} e^{-t^2/2} dt \\
& = \sum_{i=1}^{\lfloor \pi B_n \rfloor} \frac{1}{\pi B_n} \int_i^{i+1} |f_{S_n}(t) - e^{-t^2/2}| dt + \frac{1}{\pi B_n} \int_{\lfloor \pi B_n \rfloor}^{\pi B_n} |f_{S_n}(t) - e^{-t^2/2}| dt + \frac{1}{\pi B_n} \int_{\pi B_n}^{\infty} e^{-t^2/2} dt \\
& =: \Omega_1 + \Omega_2 + \Omega_3.
\end{aligned}$$

**Upper bound on  $\Omega_1$ .** For  $n = 10$  and  $\sigma^2 = 5$ , it holds  $\Omega_1 < 2.57 \times 10^{-37}$ .

Consider  $\Omega_1$  that corresponds to the case  $t \in [0, \lfloor \pi B_n \rfloor]$ . We observe that

$$\frac{\partial}{\partial t} \left( \frac{\theta_3(-i\sigma\pi t/\sqrt{n}, e^{-2\sigma^2\pi^2})}{\theta_3(0, e^{-2\sigma^2\pi^2})} \right) \begin{cases} < 0, & t < 0, \\ = 0, & t = 0, \\ > 0, & t > 0. \end{cases} \quad (\text{C.1})$$

To see this, we note that

$$\begin{aligned}
\frac{\partial}{\partial t} \left( \frac{\theta_3(-i\sigma\pi t/\sqrt{n}, e^{-2\sigma^2\pi^2})}{\theta_3(0, e^{-2\sigma^2\pi^2})} \right) &= \frac{\partial}{\partial t} \left( \frac{\sum_{k=-\infty}^{\infty} e^{-2\sigma^2\pi^2 k^2} e^{2\pi\sigma k t/\sqrt{n}}}{\theta_3(0, e^{-2\sigma^2\pi^2})} \right) \\
&= \frac{\sum_{k=-\infty}^{\infty} 2\pi\sigma k/\sqrt{n} \cdot e^{-2\sigma^2\pi^2 k^2} e^{2\pi\sigma k t/\sqrt{n}}}{\theta_3(0, e^{-2\sigma^2\pi^2})} \\
&= \frac{\sum_{k=1}^{\infty} 2\pi\sigma k/\sqrt{n} \cdot e^{-2\sigma^2\pi^2 k^2} (e^{2\pi\sigma k t/\sqrt{n}} - e^{-2\pi\sigma k t/\sqrt{n}})}{\theta_3(0, e^{-2\sigma^2\pi^2})},
\end{aligned}$$

which obviously implies Equation (C.1). By Equation (C.1), we conclude that for any  $t \in [j-1, j]$  and  $1 \leq j \leq \lfloor \pi B_n \rfloor$ , we have

$$\begin{aligned}
& e^{-t^2/2} \left| \left( \frac{\theta_3(-i\sigma\pi t/\sqrt{n}, e^{-2\sigma^2\pi^2})}{\theta_3(0, e^{-2\sigma^2\pi^2})} \right)^n - 1 \right| \\
& \leq e^{-j^2/2} \left| \left( \frac{\theta_3(-i\sigma\pi(j+1)/\sqrt{n}, e^{-2\sigma^2\pi^2})}{\theta_3(0, e^{-2\sigma^2\pi^2})} \right)^n - 1 \right|.
\end{aligned}$$

Numerically, one can verify that, for any  $1 \leq j \leq \lfloor \pi B_n \rfloor$ ,

$$\frac{1}{\pi B_n} \sum_{j=1}^{\lfloor \pi B_n \rfloor} e^{-(j-1)^2/2} \left| \left( \frac{\theta_3 \left( -i\sigma\pi j/\sqrt{n}, e^{-2\sigma^2\pi^2} \right)}{\theta_3 \left( 0, e^{-2\sigma^2\pi^2} \right)} \right)^n - 1 \right| < 2.57 \times 10^{-37}.$$

Therefore,  $\Omega_1$  can be bounded as

$$\Omega_1 = \sum_{i=1}^{\lfloor \pi B_n \rfloor} \frac{1}{\pi B_n} \int_i^{i+1} \left| f_{S_n}(t) - e^{-t^2/2} \right| dt < 2.57 \times 10^{-37}.$$

**Upper bound on  $\Omega_2$ .** For  $n = 10$  and  $\sigma^2 = 5$ , it holds  $\Omega_2 < 2.1 \times 10^{-106}$ .

To bound  $\Omega_2$ , we decompose

$$\begin{aligned} \Omega_2 &= \frac{1}{\pi B_n} \int_{\lfloor \pi B_n \rfloor}^{\pi B_n} \left| f_{S_n}(t) - e^{-t^2/2} \right| dt \\ &\leq \frac{1}{\pi B_n} \int_{\lfloor \pi B_n \rfloor}^{\pi B_n} |f_{S_n}(t)| dt + \frac{1}{\pi B_n} \int_{\lfloor \pi B_n \rfloor}^{\pi B_n} e^{-t^2/2} dt \\ &\leq \Omega_4 + \Omega_5. \end{aligned}$$

First, it is easy to see that

$$\Omega_5 \leq \frac{\pi B_n - \lfloor \pi B_n \rfloor}{\pi B_n} \cdot e^{-\lfloor \pi B_n \rfloor^2/2} < 7.65 \times 10^{-110}.$$

Thus, it is enough to estimate  $\Omega_4$  numerically as follows. Recall Proposition A.6 that implies

$$\max_{t \in [\lfloor \pi B_n \rfloor, \pi B_n]} f_{S_n}(t) = f_{S_n}(\lfloor \pi B_n \rfloor).$$

Then, numerical results show that

$$\Omega_4 \leq \frac{\pi B_n - \lfloor \pi B_n \rfloor}{\pi B_n} \cdot f_{S_n}(\lfloor \pi B_n \rfloor) < 2.02 \times 10^{-106}.$$

**Upper bound on  $\Omega_3$ .** For  $n = 10$  and  $\sigma^2 = 5$ , it holds  $\Omega_3 < 1.45 \times 10^{-110}$ .

For  $x > 0$ , the Gaussian tail bound is given by

$$\int_x^\infty e^{-s^2/2} ds \leq \frac{1}{x} e^{-x^2/2}. \tag{C.2}$$

By Equation (C.2), we have

$$\Omega_3 \leq \frac{1}{\pi B_n} \frac{e^{-(\pi B_n)^2/2}}{\pi B_n} < 1.45 \times 10^{-110}.$$

## D Omitted details of Section A.6

### D.1 Proof of Proposition A.12

Let  $\Lambda_1$  and  $\Lambda_2$  be the events defined as

$$\Lambda_1 := \bigcap_{i=1}^k \left\{ \left| \sum_{j=1}^{n_i} X_{ij} \right| \leq 12 \cdot \sigma_i \sqrt{n_i} \right\},$$

$$\Lambda_2 := \bigcap_{i=1}^k \{ |\bar{X}_i| \leq 12 \cdot \sigma_i \sqrt{n_i} \}.$$

By the triangle inequality, we have

$$\begin{aligned} & \left| \mathbb{P}_{X_{ij} \sim \mathcal{N}_{\mathbb{Z}}(0, \sigma_i^2)} \left[ \sum_{i=1}^k a_i \sum_{j=1}^{n_i} X_{ij} > t_\epsilon \right] - \nu \left( \sum_{i=1}^k a_i \bar{X}_i \geq t_\epsilon \right) \right| \\ & \leq \mathbb{P}_{X_{ij} \sim \mathcal{N}_{\mathbb{Z}}(0, \sigma_i^2)} \left[ \sum_{i=1}^k a_i \sum_{j=1}^{n_i} X_{ij} > t_\epsilon, \Lambda_1^c \right] + \nu \left( \sum_{i=1}^k a_i \bar{X}_i \geq t_\epsilon, \Lambda_2^c \right) \\ & \quad + \left| \mathbb{P}_{X_{ij} \sim \mathcal{N}_{\mathbb{Z}}(0, \sigma_i^2)} \left[ \sum_{i=1}^k a_i \sum_{j=1}^{n_i} X_{ij} > t_\epsilon, \Lambda_1 \right] - \nu \left( \sum_{i=1}^k a_i \bar{X}_i \geq t_\epsilon, \Lambda_2 \right) \right|. \end{aligned}$$

This further implies that

$$\begin{aligned} & \left| \mathbb{P}_{X_{ij} \sim \mathcal{N}_{\mathbb{Z}}(0, \sigma_i^2)} \left[ \sum_{i=1}^k a_i \sum_{j=1}^{n_i} X_{ij} > t_\epsilon \right] - \nu \left( \sum_{i=1}^k a_i \bar{X}_i \geq t_\epsilon \right) \right| \\ & \leq \mathbb{P}_{X_{ij} \sim \mathcal{N}_{\mathbb{Z}}(0, \sigma_i^2)} (\Lambda_1^c) + \nu (\Lambda_2^c) \\ & \quad + \left| \mathbb{P}_{X_{ij} \sim \mathcal{N}_{\mathbb{Z}}(0, \sigma_i^2)} \left[ \sum_{i=1}^k a_i \sum_{j=1}^{n_i} X_{ij} > t_\epsilon, \Lambda_1 \right] - \nu \left( \sum_{i=1}^k a_i \bar{X}_i \geq t_\epsilon, \Lambda_2 \right) \right| \\ & = \Omega_6 + \Omega_7 + \Omega_8. \end{aligned}$$

**Upper bound on  $\Omega_6$ .** We have

$$\mathbb{P}_{X_{ij} \sim \mathcal{N}_{\mathbb{Z}}(0, \sigma_i^2)} [\Lambda_1^c] \leq \sum_{i=1}^k \mathbb{P}_{X_{ij} \sim \mathcal{N}_{\mathbb{Z}}(0, \sigma_i^2)} \left[ \left| \frac{1}{\sqrt{n_i}} \sum_{j=1}^{n_i} X_{ij} \right| > 12 \cdot \sigma_i \right].$$

According to (A.2),  $\sum_{j=1}^{n_i} X_{ij}$  is sub-Gaussian with variance proxy  $\sqrt{n_i \sigma_i^2}$ . As a result, it holds

$$\mathbb{P}_{X_{ij} \sim \mathcal{N}_{\mathbb{Z}}(0, \sigma_i^2)} \left[ \left| \frac{1}{\sqrt{n_i}} \sum_{j=1}^{n_i} X_{ij} \right| > 12 \cdot \sigma_i \right] \leq e^{-\frac{(12)^2 n \sigma_i^2}{2 n \sigma_i^2}} = e^{-\frac{12^2}{2}}. \quad (\text{D.1})$$

Therefore, we have

$$\Omega_6 \leq k \times e^{-\frac{12^2}{2}} =: \mathcal{E}_0^{(0)}.$$

**Upper bound on  $\Omega_7$ .** Similar to the upper bound on  $\Omega_6$ , we have

$$\nu(\Lambda_2^c) \leq \sum_{i=1}^k \nu(|\bar{X}_i| > 12 \cdot \sigma_i \sqrt{n_i}).$$

Note that

$$\begin{aligned} \nu(|\bar{X}_i| > 12 \cdot \sigma_i \sqrt{n_i}) &= \sum_{\{x \in \mathbb{Z}: x > 12 \cdot \sigma_i \sqrt{n_i}\}} \frac{1}{\sqrt{n_i \sigma_i^2}} \phi\left(\frac{x}{\sqrt{n_i \sigma_i^2}}\right) \\ &= \sum_{\{x \in \mathbb{Z}: x > 12 \cdot \sigma_i \sqrt{n_i}\}} \frac{1}{\sqrt{2\pi n_i \sigma_i^2}} e^{-x^2/(2n_i \sigma_i^2)} \\ &= \frac{1}{\sqrt{2\pi n_i \sigma_i^2}} \int_{[12 \cdot \sigma_i \sqrt{n_i}]^{\infty}} e^{-x^2/(2n_i \sigma_i^2)} dx \\ &\leq \frac{1}{\sqrt{2\pi n_i \sigma_i^2}} e^{-\frac{[12 \cdot \sigma_i \sqrt{n_i}]^2}{2n_i \sigma_i^2}} < e^{-\frac{12^2}{2}}. \end{aligned}$$

Therefore, we obtain

$$\Omega_7 \leq k \times e^{-\frac{12^2}{2}} =: \mathcal{E}_1^{(0)}.$$

**Upper bound on  $\Omega_8$ .** By the independence of  $X_{ij}$  and  $\bar{X}_i$ , we immediately have

$$\begin{aligned} &\mathbb{P}_{X_{ij} \sim \mathcal{N}_{\mathbb{Z}}(0, \sigma_i^2)} \left[ \sum_{i=1}^k a_i \sum_{j=1}^{n_i} X_{ij} > t_\epsilon, \Lambda_1 \right] \\ &= \sum_{\{y_i\}_{i=1}^k \in \mathbb{Z}^k} \mathbf{1} \left( \sum_{i=1}^k a_i y_i > t_\epsilon, |y_i| \leq 12\sqrt{n_i} \sigma_i \right) \cdot \prod_{i=1}^k \mathbb{P}_{X_{ij} \sim \mathcal{N}_{\mathbb{Z}}(0, \sigma_i^2)} \left[ \sum_{j=1}^{n_i} X_{ij} = y_i \right], \end{aligned}$$

and

$$\begin{aligned} &\nu \left( \sum_{i=1}^k a_i \bar{X}_i \geq t_\epsilon, \Lambda_2 \right) \\ &= \sum_{\{y_i\}_{i=1}^k \in \mathbb{Z}^k} \mathbf{1} \left( \sum_{i=1}^k a_i y_i > t_\epsilon, |y_i| \leq 12\sqrt{n_i} \sigma_i \right) \cdot \prod_{i=1}^k \nu[\bar{X}_i = y_i] \\ &= \sum_{\{y_i\}_{i=1}^k \in \mathbb{Z}^k} \mathbf{1} \left( \sum_{i=1}^k a_i y_i > t_\epsilon, |y_i| \leq 12\sqrt{n_i} \sigma_i \right) \cdot \prod_{i=1}^k \frac{1}{\sqrt{n_i \sigma_i^2}} \phi\left(\frac{y_i}{\sqrt{n_i \sigma_i^2}}\right). \end{aligned}$$

Recall the definition of  $\Omega_8$ . It holds

$$\begin{aligned}
& \left| \mathbb{P}_{X_{ij} \sim \mathcal{N}_{\mathbb{Z}}(0, \sigma_i^2)} \left[ \sum_{i=1}^k a_i \sum_{j=1}^{n_i} X_{ij} > t_\epsilon, \Lambda_1 \right] - \nu \left( \sum_{i=1}^k a_i \bar{X}_i \geq t_\epsilon, \Lambda_2 \right) \right| \\
& \leq \sum_{\{y_i\}_{i=1}^k \in \mathbb{Z}^k} \mathbf{1} \left( \sum_{i=1}^k a_i y_i > t_\epsilon, |y_i| \leq 12\sqrt{n_i} \sigma_i \right) \cdot \left| \prod_{i=1}^k \mathbb{P}_{X_{ij} \sim \mathcal{N}_{\mathbb{Z}}(0, \sigma_i^2)} \left[ \sum_{j=1}^{n_i} X_{ij} = y_i \right] - \prod_{i=1}^k \frac{1}{\sqrt{n_i \sigma_i^2}} \phi \left( \frac{y_i}{\sqrt{n_i \sigma_i^2}} \right) \right| \\
& < \sum_{\{y_i\}_{i=1}^k \in \mathbb{Z}^k} \mathbf{1} (-12\sqrt{n_i} \sigma_i \leq y_i \leq 12\sqrt{n_i} \sigma_i) \cdot \left| \prod_{i=1}^k \mathbb{P}_{X_{ij} \sim \mathcal{N}_{\mathbb{Z}}(0, \sigma_i^2)} \left[ \sum_{j=1}^{n_i} X_{ij} = y_i \right] - \prod_{i=1}^k \frac{1}{\sqrt{n_i \sigma_i^2}} \phi \left( \frac{y_i}{\sqrt{n_i \sigma_i^2}} \right) \right| \\
& \leq \sum_{\{y_i\}_{i=1}^k \in \mathbb{Z}^k} \mathbf{1} (-12\sqrt{n_i} \sigma_i \leq y_i \leq 12\sqrt{n_i} \sigma_i) \\
& \quad \cdot \max_{\{y_i\}_{i=1}^k \in \mathbb{Z}^k} \left| \prod_{i=1}^k \mathbb{P}_{X_{ij} \sim \mathcal{N}_{\mathbb{Z}}(0, \sigma_i^2)} \left[ \sum_{j=1}^{n_i} X_{ij} = y_i \right] - \prod_{i=1}^k \frac{1}{\sqrt{n_i \sigma_i^2}} \phi \left( \frac{y_i}{\sqrt{n_i \sigma_i^2}} \right) \right|.
\end{aligned}$$

Note that for two sequences  $\{c_i\}_{i=1}^k$  and  $\{b_i\}_{i=1}^k$ , we have

$$\begin{aligned}
\left| \prod_{i=1}^k c_i - \prod_{i=1}^k b_i \right| &= \left| \sum_{i=1}^k \left[ \left( \prod_{j=1}^{i-1} c_j \right) (c_i - b_i) \left( \prod_{j=i+1}^k b_j \right) \right] \right| \\
&\leq \sum_{i=1}^k |c_i - b_i| \cdot \left| \left( \prod_{j=1}^{i-1} c_j \right) \left( \prod_{j=i+1}^k b_j \right) \right|.
\end{aligned}$$

Therefore, let

$$\begin{aligned}
c_i &= \mathbb{P}_{X_{ij} \sim \mathcal{N}_{\mathbb{Z}}(0, \sigma_i^2)} \left[ \sum_{j=1}^{n_i} X_{ij} = y_i \right] \leq \frac{1}{\sqrt{n_i \sigma_i^2}} \phi \left( \frac{y_i}{\sqrt{n_i \sigma_i^2}} \right) + r_{n_i, \sigma_i} \leq \frac{1}{\sqrt{2\pi n_i \sigma_i^2}} + r_{n_i, \sigma_i}, \\
b_i &= \frac{1}{\sqrt{n_i \sigma_i^2}} \phi \left( \frac{y_i}{\sqrt{n_i \sigma_i^2}} \right) \leq \frac{1}{\sqrt{2\pi n_i \sigma_i^2}},
\end{aligned}$$

and we have

$$\begin{aligned}
& \left| \mathbb{P}_{X_{ij} \sim \mathcal{N}_{\mathbb{Z}}(0, \sigma_i^2)} \left[ \sum_{i=1}^k a_i \sum_{j=1}^{n_i} X_{ij} > t_\epsilon, \Lambda_1 \right] \right. \\
& \quad \left. - \sum_{\{y_i\}_{i=1}^k \in \mathbb{Z}^k} \mathbf{1} \left( \sum_{i=1}^k a_i y_i > t_\epsilon, |y_i| \leq 12\sqrt{n_i} \sigma_i \right) \cdot \prod_{i=1}^k \frac{1}{\sqrt{n_i \sigma_i^2}} \phi \left( \frac{y_i}{\sqrt{n_i \sigma_i^2}} \right) \right| \\
& \leq \prod_{i=1}^k (24\sqrt{n_i} \sigma_i) \cdot \sum_{i=1}^k r_{n_i, \sigma_i} \cdot \max_{\{y_j\}_{j=1}^k \in \mathbb{Z}^k} \left| \left( \prod_{j=1}^{i-1} c_j \right) \left( \prod_{j=i+1}^k b_j \right) \right|. \tag{D.2}
\end{aligned}$$

Overall, we obtain

$$\Omega_9 \leq \prod_{i=1}^k (24\sqrt{n_i}\sigma_i) \cdot \sum_{i=1}^k r_{n_i, \sigma_i} \cdot \max_{\{y_j\}_{j=1}^k \in \mathbb{Z}^k} \left| \left( \prod_{j=1}^{i-1} c_j \right) \left( \prod_{j=i+1}^k b_j \right) \right| =: \mathcal{E}_2^{(0)}.$$

This completes the proof of Proposition A.12.

## D.2 Proof of Proposition A.13

Let  $L = 10^3$ . For all  $a_i L \in \mathbb{Z}$  with  $a_i$  given in Table 3, we have

$$\nu \left( \sum_{i=1}^k a_i \bar{X}_i \geq t_\epsilon \right) = \sum_{m \geq t_\epsilon L} \nu \left( \sum_{i=1}^k a_i L \bar{X}_i = m \right) = \sum_{6 \times t_\epsilon L \geq m \geq t_\epsilon L} \nu \left( \sum_{i=1}^k a_i L \bar{X}_i = m \right) + \mathcal{E}^{(1)},$$

where

$$\mathcal{E}^{(1)} = \nu \left( \sum_{i=1}^k a_i L \bar{X}_i > 6 \times t_\epsilon L \right) \leq \sum_{i=1}^k \nu \left( \bar{X}_i > \frac{6 \times t_\epsilon L}{k \cdot L \cdot a_i} \right).$$

By discrete Fourier transform (Exercise 3.3.2 (iii) in Durrett (2019)), we have

$$\begin{aligned} & \sum_{6t_\epsilon L \geq m \geq t_\epsilon L} \nu \left( \sum_{i=1}^k a_i L \bar{X}_i = m \right) \\ &= \sum_{6t_\epsilon L \geq m \geq t_\epsilon L} \frac{1}{2\pi} \int_{-\pi}^{\pi} e^{-itm} \prod_{i=1}^k f_{a_i L \bar{X}_i}(t) dt = \frac{1}{\pi} \int_0^{\pi} \sum_{6t_\epsilon L \geq m \geq t_\epsilon L} \cos(tm) \prod_{i=1}^k f_{a_i L \bar{X}_i}(t) dt \\ &= \frac{1}{2\pi} \int_0^{\pi} \left[ \cos(\lceil t_\epsilon L \rceil \cdot t) + \cos(\lceil 6t_\epsilon L \rceil \cdot t) + \frac{\cos(t/2)}{\sin(t/2)} (\sin(\lceil 6t_\epsilon L \rceil \cdot t) - \sin(\lceil t_\epsilon L \rceil \cdot t)) \right] \prod_{i=1}^k f_{\bar{X}_i}(a_i L t) dt, \end{aligned} \tag{D.3}$$

where  $f_{a_i L \bar{X}_i}(t)$  and  $f_{\bar{X}_i}(t)$  are the characteristic functions of  $a_i L \cdot \bar{X}_i$  and  $\bar{X}_i$ , correspondingly. The closed-form representation of the  $f_{a_i L \bar{X}_i}$  is given by

$$\begin{aligned} f_{a_i L \bar{X}_i}(t) &= f_{\bar{X}_i}(a_i L t) = \sum_{u=-\infty}^{\infty} e^{iua_i L t} \frac{e^{-\frac{u^2}{2} \cdot \frac{1}{n_i \sigma_i^2}}}{\sqrt{2\pi n_i \sigma_i^2}} \\ &= \frac{1}{\sqrt{2\pi n_i \sigma_i^2}} + 2 \sum_{u=1}^{\infty} \cos(ua_i L t) \cdot \frac{e^{-\frac{u^2}{2} \cdot \frac{1}{n_i \sigma_i^2}}}{\sqrt{2\pi n_i \sigma_i^2}}. \end{aligned}$$

Similar results hold if we replace  $t_\epsilon$  with  $T_\epsilon = \frac{n}{2} \left( \frac{\epsilon}{\rho} + 1 \right)$ .

### D.3 Calculation of Fact A.14

First, we have

$$\begin{aligned} & \left| \frac{1}{2} \left[ \cos(\lceil t_\epsilon L \rceil \cdot t) + \cos(\lceil 6t_\epsilon L \rceil \cdot t) + \frac{\cos(t/2)}{\sin(t/2)} (\sin(\lceil 6t_\epsilon L \rceil \cdot t) - \sin(\lceil t_\epsilon L \rceil \cdot t)) \right] \right| \\ &= \left| \sum_{6 \times t_\epsilon L \geq m \geq t_\epsilon L} \cos(tm) \right| \leq 5t_\epsilon L < 1.3 \times 10^5. \end{aligned}$$

Let  $c$  be a constant such that  $|f_{\bar{X}_i}(a_i Lt)| = |e^{i\bar{X}_i a_i Lt}| \leq c$ . Then, it holds

$$\left| \prod_{i=1}^k f_{\bar{X}_i}(a_i Lt) \right| = \left| \prod_{i=1}^k f_{a_i L \bar{X}_i}(t) \right| \leq c^{k-1} \cdot \min \{ |f_{\bar{X}_1}(a_1 Lt)|, \dots, |f_{\bar{X}_k}(a_k Lt)| \}.$$

Numerically, one can verify that  $c < 1 + 1.0 \times 10^{-50}$ . Output of Characteristic Function Evaluation in GitHub records the numerical value of  $\{f_{\bar{X}_1}(a_1 Lt), \dots, f_{\bar{X}_k}(a_k Lt)\}$  for all  $t \in \Lambda$  with  $\Lambda$  given by

$$\Lambda = \left\{ \frac{j}{200} \times \frac{\pi}{a_i L} : 0 \leq j \leq 200 \times a_i L, 1 \leq i \leq k \right\}.$$

Recall Proposition A.6 that  $f_{\bar{X}_i}(a_i Lt)$  is a  $2\pi/(a_i L)$ -periodic function and monotone within any  $\left[ k \times \frac{\pi}{a_i L}, (k+1) \times \frac{\pi}{a_i L} \right]$ ,  $k \in \mathbb{Z}$ . Inspired by the Sieve Method from number theory, we make the following observations in the order of decreasing  $\sigma_i^2$ :

$$\begin{aligned} \left| \prod_{i=1}^k f_{\bar{X}_i}(a_i Lt) \right| &< c^{k-1} \cdot f_{\bar{X}_7}(a_7 Lt) < 10^{-35}, \quad \text{for } t \in [0.062831853, 2.031563249] \cup [2.157226955, \pi]. \\ \left| \prod_{i=1}^k f_{\bar{X}_i}(a_i Lt) \right| &< c^{k-1} \cdot f_{\bar{X}_1}(a_1 Lt) < 10^{-35}, \quad \text{for } t \in [0.024347343, 0.062831853] \cup [2.031039651, 2.158274153]. \\ \left| \prod_{i=1}^k f_{\bar{X}_i}(a_i Lt) \right| &< c^{k-1} \cdot f_{\bar{X}_3}(a_3 Lt) < 10^{-35}, \quad \text{for } t \in [0.011827172, 0.024578343]. \\ \left| \prod_{i=1}^k f_{\bar{X}_i}(a_i Lt) \right| &< c^{k-1} \cdot f_{\bar{X}_2}(a_2 Lt) < 10^{-35}, \quad \text{for } t \in [0.006592758, 0.011866965]. \end{aligned}$$

Therefore, we conclude for all  $t \in [0.006592758, \pi] \subset [1/100, \pi]$ , it holds

$$\left| \prod_{i=1}^k f_{\bar{X}_i}(a_i Lt) \right| < 10^{-35},$$

which further implies that

$$\mathcal{E}^{(2)} < \frac{1}{\pi} \times \pi \times 10^{-35} \times 1.3 \times 10^5 < 1.3 \times 10^{-30}.$$



#### D.4 Calculation of Fact A.15

Recall (D.3) that,

$$F(t) = \frac{1}{\pi} \sum_{6t_\epsilon L \geq m \geq t_\epsilon L} \cos(tm) \mathbb{E} e^{itX} = \frac{1}{\pi} \sum_{6t_\epsilon L \geq m \geq t_\epsilon L} \mathbb{E} \cos(tm) \cos(tX),$$

where  $X = a_1 L \bar{X}_1 + \dots + a_k L \bar{X}_k$ .

**Moments of  $X$ .** We compute the moments of  $X$  using the triangle inequality

$$\|X\|_{L_p}^p \leq (\|a_1 L \bar{X}_1\|_{L_p} + \dots + \|a_k L \bar{X}_k\|_{L_p})^p.$$

Moreover, numerically, it holds  $\mathbb{E}|X| \leq 7.0 \times 10^3$ ,  $\mathbb{E}|X|^2 \leq 7.6 \times 10^7$ ,  $\mathbb{E}|X|^3 \leq 1.1 \times 10^{12}$ ,  $\mathbb{E}|X|^4 \leq 1.8 \times 10^{16}$ ,  $\mathbb{E}|X|^5 \leq 3.3 \times 10^{20}$ ,  $\mathbb{E}|X|^6 \leq 6.6 \times 10^{24}$ .

**Upper Bound on 6-th order differentiation of  $F(t)$ .** The 6-th order differentiation of  $F(t)$  is bounded as follows.

$$\begin{aligned} \sup_t \left| F^{(6)}(t) \right| &\leq \frac{1}{\pi} \cdot \sum_{6t_\epsilon L \geq m \geq t_\epsilon L} \left| \frac{d^6}{dt^6} \mathbb{E} \cos(tm) \cos(tX) \right| \\ &= \sum_{6t_\epsilon L \geq m \geq t_\epsilon L} \mathbb{E} \left| 2mX (3m^4 + 10m^2 X^2 + 3X^4) \sin(tm) \sin(tX) \right. \\ &\quad \left. - (m^6 + 15m^4 X^2 + 15m^2 X^4 + X^6) \cos(tm) \cos(tX) \right| \\ &\leq \frac{1}{\pi} \cdot \sum_{6t_\epsilon L \geq m \geq t_\epsilon L} m^6 + 6m^5 \mathbb{E}|X| + 15m^4 \mathbb{E}X^2 + 20m^3 \mathbb{E}|X|^3 + 15m^2 \mathbb{E}X^4 + 6m \mathbb{E}|X|^5 + \mathbb{E}|X|^6 \\ &\leq \frac{1}{\pi} \cdot \sum_{6t_\epsilon L \geq m \geq t_\epsilon L} m^6 + 6m^5 (7.0 \times 10^3) + 15m^4 (7.6 \times 10^7) \\ &\quad + 20m^3 (1.1 \times 10^{12}) + 15m^2 (1.8 \times 10^{16}) + 6m (3.3 \times 10^{20}) + (6.6 \times 10^{24}) \\ &< \frac{1}{\pi} \times 3.54 \times 10^{35} = 1.2 \times 10^{35}. \end{aligned}$$

**Boole's sum and error bound.** Consider the integral  $\int_a^b F(x) dx$ . Let  $\{x_i\}_{i=1}^N$  be a partition of  $[a, b]$  with

$$x_i := a + i * h, \quad h = \frac{b-a}{N-1},$$

for  $i = 0, \dots, N-1$ . Consider the following discretization of the integration.

$$\begin{aligned} &\sum_{l=1}^{\frac{N-1}{4}} \frac{2h}{45} \times (7F(x_{4l-4}) + 32F(x_{4l-3}) + 12F(x_{4l-2}) + 32F(x_{4l-1}) + 7F(x_{4l})) \\ &= \frac{2h}{45} \times \left[ 7(F(a) + F(b)) + \sum_{k=1}^{(N-1)/4} (32F(x_{4k-3}) + 12F(x_{4k-2}) + 32F(x_{4k-1})) + 14 \times \sum_{k=1}^{m-1} F(x_{4k}) \right]. \end{aligned}$$

Equation 3.2 in [Sablonnière et al. \(2010\)](#) indicates that the error is bounded as

$$\left| \int_a^b F(t) dt - \sum_{k=1}^{\frac{N-1}{4}} \frac{2h}{45} \times (7F(x_{4l-4}) + 32F(x_{4l-3}) + 12F(x_{4l-2}) + 32F(x_{4l-1}) + 7F(x_{4l})) \right|$$

$$\leq \frac{2}{945} \cdot \max_{t \in [a,b]} f^{(6)}(t) \cdot h^6 \cdot (b-a).$$

In our numerical results, we set  $h = \frac{1}{100 \times 10^7}$ ,  $a = 0$ , and  $b = \frac{1}{100}$ . Therefore, the error bound is given by

$$\left| \int_0^{\frac{1}{100}} F(t) dt - \sum_{k=1}^{\frac{N-1}{4}} \frac{2h}{45} \times (7F(x_{4l-4}) + 32F(x_{4l-3}) + 12F(x_{4l-2}) + 32F(x_{4l-1}) + 7F(x_{4l})) \right|$$

$$\leq \frac{2}{945} \times 1.2 \times 10^{35} \times \frac{1}{100} \times \left( \frac{1}{100 \times 10^7} \right)^6$$

$$< 2.54 \times 10^{-24}.$$